Circulation

American Heart Association®

Hemopexin Therapy Improves Cardiovascular Function by Preventing Heme-Induced Endothelial Toxicity in Mouse Models of Hemolytic Diseases

Francesca Vinchi, Lucia De Franceschi, Alessandra Ghigo, Tim Townes, James Cimino, Lorenzo Silengo, Emilio Hirsch, Fiorella Altruda and Emanuela Tolosano

The online version of this article, along with updated information and services, is located on the
World Wide Web at:
http://circ.ahajournals.org/content/127/12/1317

Data Supplement (unedited) at:
http://circ.ahajournals.org/content/suppl/2013/02/27/CIRCULATIONAHA.112.130179.DC1.html

Permissions: Requests for permissions to reproduce figures, tables, or portions of articles originally published in *Circulation* can be obtained via RightsLink, a service of the Copyright Clearance Center, not the Editorial Office. Once the online version of the published article for which permission is being requested is located, click Request Permissions in the middle column of the Web page under Services. Further information about this process is available in the Permissions and Rights Question and Answer document.

Reprints: Information about reprints can be found online at:
http://www.lww.com/reprints

Subscriptions: Information about subscribing to *Circulation* is online at:
http://circ.ahajournals.org//subscriptions/

Hemopexin Therapy Improves Cardiovascular Function by Preventing Heme-Induced Endothelial Toxicity in Mouse Models of Hemolytic Diseases

Francesca Vinchi, PhD; Lucia De Franceschi, MD; Alessandra Ghigo, PhD; Tim Townes, PhD;
James Cimino, BSc; Lorenzo Silengo, MD; Emilio Hirsch, PhD; Fiorella Altruda, PhD;
Emanuela Tolosano, PhD

Background—Hemolytic diseases are characterized by enhanced intravascular hemolysis resulting in heme-catalyzed reactive oxygen species generation, which leads to endothelial dysfunction and oxidative damage. Hemopexin (Hx) is a plasma heme scavenger able to prevent endothelial damage and tissue congestion in a model of heme overload. Here, we tested whether Hx could be used as a therapeutic tool to counteract heme toxic effects on the cardiovascular system in hemolytic diseases.

Methods and Results—By using a model of heme overload in Hx-null mice, we demonstrated that heme excess in plasma, if not bound to Hx, promoted the production of reactive oxygen species and the induction of adhesion molecules and caused the reduction of nitric oxide availability. Then, we used β-thalassemia and sickle cell disease mice as models of hemolytic diseases to evaluate the efficacy of an Hx-based therapy in the treatment of vascular dysfunction related to heme overload. Our data demonstrated that Hx prevented heme-iron loading in the cardiovascular system, thus limiting the production of reactive oxygen species, the induction of adhesion molecules, and the oxidative inactivation of nitric oxide synthase/nitric oxide, and promoted heme recovery and detoxification by the liver mainly through the induction of heme oxygenase activity. Moreover, we showed that in sickle cell disease mice, endothelial activation and oxidation were associated with increased blood pressure and altered cardiac function, and the administration of exogenous Hx was found to almost completely normalize these parameters.

Conclusions—Hemopexin treatment is a promising novel therapy to protect against heme-induced cardiovascular dysfunction in hemolytic disorders. (***Circulation***. 2013;127:1317-1329.)

Key Words: anemia, sickle cell ■ endothelium ■ heme ■ hemopexin ■ nitric oxide ■ reactive oxygen species ■ thalassemia

Hemolytic diseases characterized by intravascular hemolysis are associated with a state of endothelial dysfunction leading to vasomotor instability and ultimately producing a proliferative vasculopathy.[1] Enhanced expression of adhesion molecules on the endothelial wall, high levels of circulating proinflammatory cytokines and activated leukocytes, pro-oxidant stress, and coagulopathy have been reported in patients suffering from several hemolytic diseases, including paroxysmal nocturnal hemoglobinuria, sickle cell disease (SCD), thalassemias, and hereditary spherocytosis.[2–4] Oxidative stress plays a central role in promoting vascular inflammation, primarily through the induction of adhesion molecules on the vascular endothelium and the promotion of monocyte and neutrophil activation.[5,6]

Clinical Perspective on p 1329

Heme represents a major source of reactive oxygen species (ROS) in hemolytic patients. Because of enhanced rates of red blood cell hemolysis, the endothelium of these patients is exposed to high levels of ROS catalyzed by plasma hemoglobin, heme, and free iron.[7,8] High levels of ROS lead to lipid, protein, and DNA damage and eventually to cell death, and they favor endothelial activation[6–9] and leukocyte recruitment, thus promoting a chronic inflammatory state.[10] In these hemolytic anemias, the presence of circulating free hemoglobin that avidly buffers nitric oxide (NO) and the generation of ROS that oxidatively inactivate NO result in reduced bioavailability of the main biovasodilator NO and abnormal vascular homeostasis, leading to endothelial dysfunction.[1,11]

Mammals have evolved a tissue and vasculoprotective program of heme metabolism that includes the plasma hemoglobin (Hb)/heme scavengers haptoglobin and hemopexin (Hx) and

the cellular enzyme heme oxygenase (HO)-1.[12–14] Haptoglobin and Hx, by binding with high-affinity Hb and heme, respectively, block their pro-oxidant effect. HO-1 degrades the heme ring into iron, carbon monoxide, and biliverdin,[15] thus exerting primary anti-inflammatory, antioxidant, and antiapoptotic effects.[12,13,16] In hemolytic diseases, the high rate of hemolysis results in the saturation and depletion of the plasma Hb/heme scavenging systems[17] and leads to a buildup of Hb and heme in the circulation that mediates pro-oxidant and proinflammatory effects on vessel endothelial cells.[18]

Although many mechanisms contribute to the complex pathophysiology of hemolytic diseases as SCD and β-thalassemia, a unifying theme is represented by the dysfunction of the vascular endothelium and the highly pro-oxidant plasma environment.[1,19–22]

SCD is characterized by recurring episodes of painful vaso-occlusion, leading to ischemia/reperfusion injury and organ damage.[6,23] Endothelial dysfunction, inflammation, and activated monocytes, neutrophils, platelets, and dense red cells all contribute to sickle cell crisis.[4,23] β -Thalassemia is frequently complicated by thromboembolic events resulting from coagulation abnormalities and damaged red cells exposing phosphatidylserine, to which endothelial activation and oxidative stress strongly contribute.[3,23,24] Moreover, severe forms of SCD and β-thalassemia require a blood transfusion regimen that further increases the amount of circulating Hb/heme, thus exacerbating oxidative stress.[25,26] Although an iron chelation therapy is routinely associated with a transfusion regimen,[27,28] no heme chelation therapy has been developed to date that specifically prevents heme-induced endothelial damage and oxidative stress.

We previously showed that heme-overloaded Hx-null mice suffered from endothelial damage and vascular congestion, thus highlighting the critical role of Hx in preventing vascular damage.[29] Therefore, we hypothesized that Hx could be administered as a drug in hemolytic diseases to prevent heme-driven endothelial dysfunction and oxidative injury. To test this hypothesis, we chose 2 mouse models of SCD and β-thalassemia,[30–32] and we evaluated the effect of an Hx-based therapy in these animals.

Our findings support the hypothesis that the replenishment of the plasma Hx pool by exogenous Hx administration is beneficial in preventing endothelial dysfunction and ameliorating the vasculopathy in hemolytic disorders.

Methods

Mice Treatment

Hx-null mice, knock-in sickle hemoglobin (HbS) SCD mice, and Hbb^th1/th1 β-thalassemia mice were described previously.[30–33] SV129 wild-type and Hx-null mice were injected in the tail vein with 30 μmol/kg freshly prepared hemin. Hx treatment in SCD and β-thalassemic mice was performed by injecting 700 μg purified human Hx (Athens Research) intraperitoneally twice a week for 1 month beginning at 1 month of age. All experiments were approved by the animal studies committee of the University of Torino (Italy).

Cell Treatment

Hemin chloride was dissolved in dimethyl sulfoxide to obtain a 4-mmol/L stock solution, diluted, and mixed 1:1 with human serum albumin (Sigma-Aldrich) or Hx. Human umbilical vein endothelial cells (HUVECs) and primary hepatocytes were treated with heme-albumin or heme-Hx 5 to 10 μmol/L in culture medium.

Heme and Iron Content

Heme content in tissues and bile was quantified fluorometrically by the method of Sassa. Tissue non–heme-iron content was determined by a colorimetric method using 4,7-diphenyl-1, 10-phenantroline disulfonic acid (Sigma) as chromogen.

Lipid Peroxidation Assay

Lipid peroxidation from tissue extracts was measured with the colorimetric assay kit Bioxytech LPO-586 from Oxis International (Portland, OR)[29] according to the manufacturer's instructions.

HO Activity Assay

HO activity was measured by spectrophotometric determination of bilirubin produced from hemin added as substrate.

ROS Production Assay

Accumulation of ROS in HUVECs and aortic rings was assessed by use of the fluorescent oxidant-sensitive dye 29,79-dichlorodihydrofluoroscein diacetate (H_2DCFDA; Molecular Probes, Eugene, OR).

Annexin V/Propidium Iodide Staining

After treatment, HUVECs were double stained with fluorescein isothiocyanate–conjugated annexin V and propidium iodide for 15 minutes at room temperature and then analyzed by flow cytometer.

NO Synthase Activity Assay

Activity of NO synthase (NOS) in liver and aorta extracts was determined by monitoring the conversion of L-[³H]arginine to L-[³H]citrulline with the NOS Activity Assay Kit N.781001 (Cayman Chemical Company). The reaction was performed following the manufacturer's instructions. Results were expressed as picomoles of citrulline per minute per gram of tissue.

Blood Pressure Measurement

Heart rate and systolic, diastolic, and mean blood pressures were measured in conscious mice with a noninvasive computerized tail cuff system (CODA, Kent Scientific Corp).

Echocardiography

Mice were anesthetized with 1% isoflurane and analyzed with a Vevo770 High Resolution Imaging System (Visual Sonics Inc, Toronto, ON, Canada). Echocardiographic parameters were measured in the long-axis M mode. Cardiac function was assessed when the heart rate was 500 to 600 bpm.

Statistical Analysis

Results were expressed as mean±SEM. Comparisons between 2 groups were performed with 2-sided Welch *t* tests and among >2 groups with 1- or 2-way ANOVA (with repeated measures when the same mice are measured in different conditions) followed by the Bonferroni posttest. Specific comparisons were performed by reverting to *t* tests and adjusting the *P* values with Bonferroni correction. The statistical tests and the numbers of comparisons used for each panel of each figure are reported in Table I in the online-only Data Supplement. A value of $P<0.05$ was considered significant.

Further details on methods are reported in the online-only Data Supplement.

Results

β-Thalassemic and SCD Mice Show Vascular Dysfunction Associated With Hx Depletion and Serum Heme Overload

Both β-thalassemia and SCD patients experience a condition of vascular dysfunction.[1] We confirmed that this also occurred

in mouse models of these diseases. Both β-thalassemic and SCD mice showed evident signs of increased endothelial activation, enhanced oxidative stress, reduced NO bioavailability, and inflammation (Figure 1A–1D), hallmarks of vascular dysfunction. The phenotype of thalassemic and SCD mice resembles that of heme-overloaded Hx-null mice, showing increased endothelial activation and oxidative stress, altered vascular permeability, inflammation,[29] and vascular antioxidant response hyperactivation (not shown). The comparison suggests that in β-thalassemia and SCD, heme overload consequent to hemolysis and plasma Hb and heme scavengers consumption may contribute to the observed vasculopathy and indicates that, although these pathologies have specific clinical outcomes, they share hemoglobinemia-related sequelae.[2] Consistently, in the serum of both thalassemic and SCD mice, haptoglobin and Hx were almost completely depleted (Figure 1E), as occurs in human patients.[17] This was associated with a significant increase in serum heme levels (thalassemic, 75 versus 20 µmol/L; SCD, 110 versus 55 µmol/L; Figure 1F).

The Lack of Hx Favors Heme Loading in the Vascular Endothelium

To understand how heme overload consequent to Hx consumption may concur to vascular dysfunction, we took advantage of the model of heme-overloaded Hx-null mice that, as reported in the previous section, mimics the Hx depletion and serum heme overload occurring in β-thalassemia and SCD.

Quantification of the heme content in the aortas from wild-type and Hx-null mice injected intravenously with 35 µmol/kg hemin revealed that in the absence of Hx, a greater amount of heme accumulated in vessels (Figure 2A). Consistently, the heme-degrading enzyme HO-1, as well as L-ferritin and ferroportin, involved in heme-derived iron storage and export, respectively, was induced to a higher extent in the aorta of heme-treated Hx-null mice than in that of the wild-type counterpart (Figure 2B–2D). Heme overload in vessels of Hx-null mice was associated with an enhanced induction of vascular cell adhesion molecule-1 and a strong increase in intracellular ROS (Figure 2E–2G).

NOS activity was significantly reduced in aortas from heme-treated Hx-null mice but not in the wild-type counterpart, suggesting reduced NO production in Hx-null endothelium (Figure 2H). Moreover, nitrotyrosine formation was significantly higher in both the aorta and serum of Hx-null mice compared with wild-type mice after heme injection, suggesting an oxidative consumption of NO and indicating an increased production of reactive nitrogen species in the absence of Hx (Figure 2I and 2L).
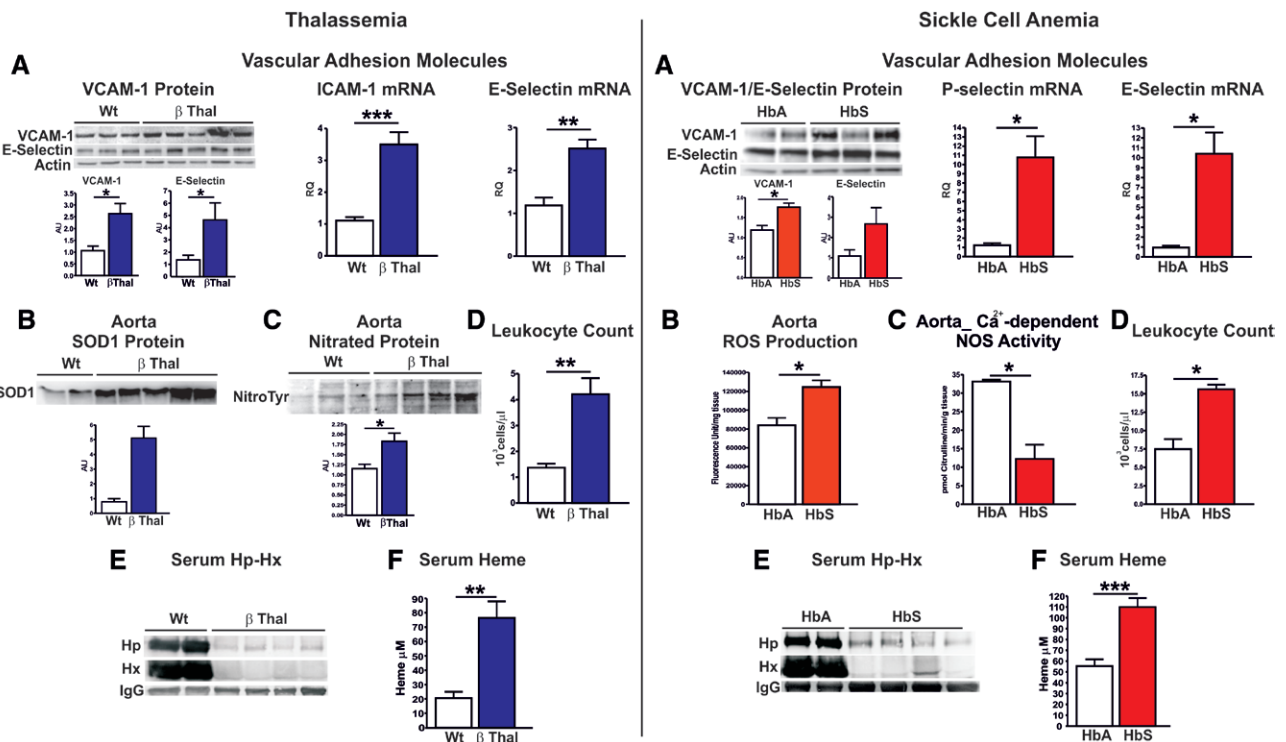
Figure 1. β-Thalassemic (β-Thal) and sickle cell disease (SCD) mice show vasculopathy associated with hemopexin (Hx) depletion and serum heme overload. Data on wild-type (Wt) and β-Thal mice and normal hemoglobin (HbA) and sickle hemoglobin (HbS) mice are shown on the **left** and **right**, respectively. **A**, Endothelial activation in β-Thal and HbS mice. Western blot showing vascular cell adhesion molecule-1 (VCAM-1) and E-selectin protein expression in aorta and quantitative reverse transcription–polymerase chain reaction analysis showing intercellular adhesion molecule-1 (ICAM-1)/P-selectin and E-selectin mRNA levels in liver. AU indicates arbitrary units; and RQ, relative quantity. **B**, Oxidative stress in vessels of β-Thal and HbS mice as evinced by superoxide dismutase 1 (SOD1) protein expression and reactive oxygen species (ROS) production. **C**, Reduced availability of active nitric oxide (NO) in vessels of β-Thal and HbS mice as demonstrated by an increased amount of nitrated proteins and reduced NO synthase (NOS) activity. **D**, Increased inflammation in β-Thal and HbS mice demonstrated by increased leukocyte number. **E** and **F**, Representative Western blots showing haptoglobin (Hp), Hx, and heme content in the serum of β-Thal and HbS mice. Wild type (Wt), HbA, n=4; β-Thal, HbS, n=8. Values represent mean±SEM. *P<0.05; **P<0.01; ***P<0.001.
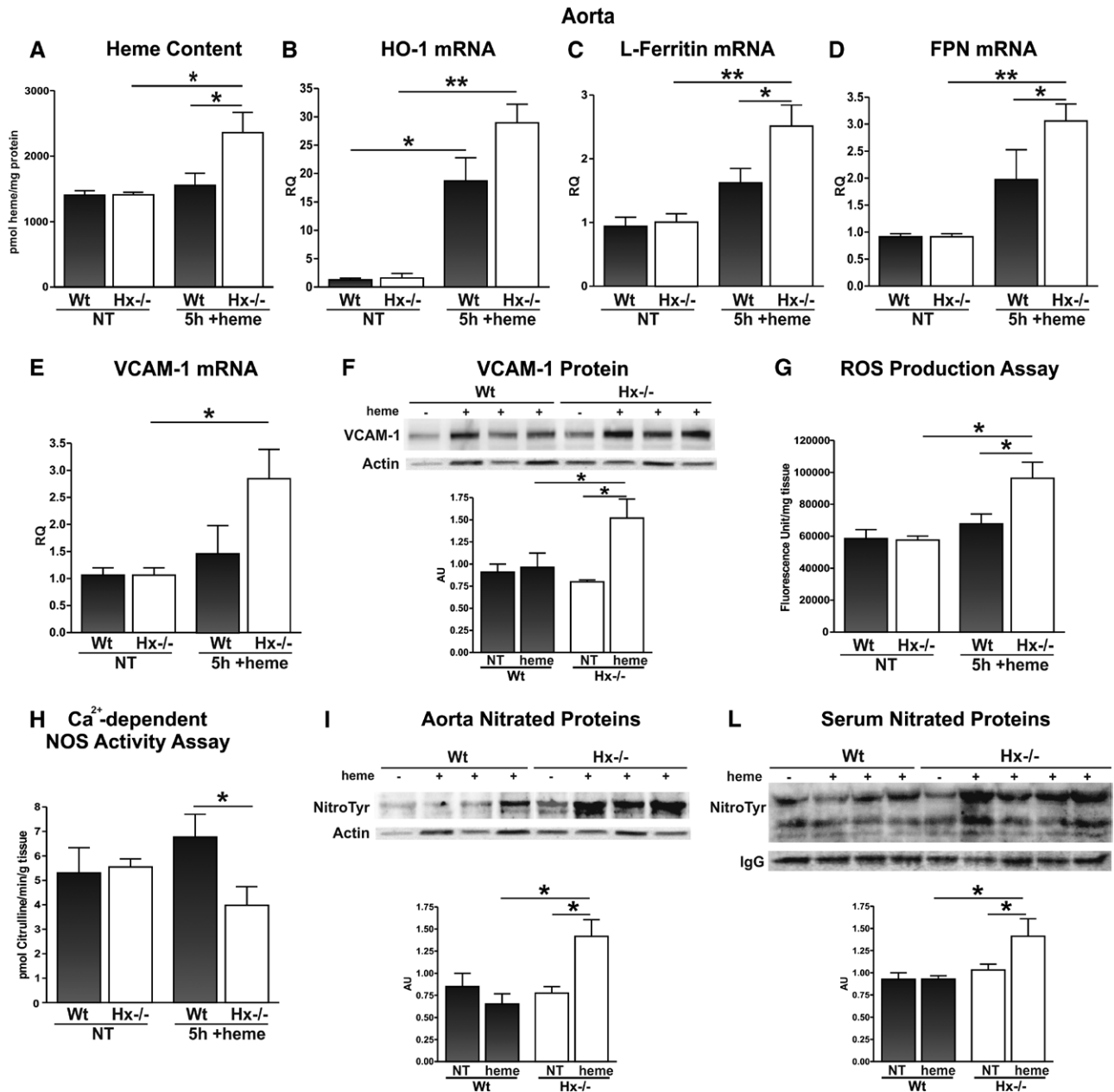
Figure 2. The lack of hemopexin (Hx) favors heme loading in the vascular endothelium. **A**, Heme content in aorta of wild-type and Hx-null mice 5 hours after heme injection (not-treated [NT], n=4; heme, n=5). **B** through **E**, Quantitative reverse transcription–polymerase chain reaction analysis of heme oxygenase-1 (HO-1), L-ferritin, ferroportin (FPN), and vascular cell adhesion molecule-1 (VCAM-1) mRNA levels in the aorta of wild-type (Wt) and Hx-null mice 5 hours after heme injection (NT, n=4; heme, n=5). **F**, Representative Western blot showing VCAM-1 expression, (**G**) reactive oxygen species (ROS) production assay (NT, n=6; heme, n=9), and (**H**) nitric oxide synthase (NOS) activity (NT, n=3; heme, n=5) in aorta from Wt and Hx-null mice 5 hours after heme injection. **I** and **L**, Representative Western blots showing nitrotyrosine formation in aorta and serum from Wt and Hx-null mice 5 hours after heme injection (NT, n=3; heme, n=5). Results shown are representative of 3 independent experiments. Values represent mean±SEM. *$P<0.05$; **$P<0.01$.

Hx Limits Heme Uptake by Endothelial Cells

Data in the previous section strongly support the conclusion that Hx limits heme uptake by the vascular endothelium. To demonstrate this, we measured heme uptake in HUVECs incubated with 7.5 µmol/L heme bound to albumin or Hx in a 1:1 ratio. After 30 minutes of incubation, heme levels were significantly higher in HUVECs treated with albumin-heme than in those treated with Hx-heme (Figure 3A), proving that Hx strongly limits heme uptake by endothelial cells. Consistent with in vivo findings, incubation of HUVECs

with Hx-heme blunted the upregulation of HO-1, L-ferritin, and ferroportin (Figure 3B–3D), as well as the induction of adhesion molecules such as intercellular adhesion molecule-1 and E-selectin, compared with incubation with albumin-heme (Figure 3E and 3F). Furthermore, treating HUVECs with the Hx-heme complex slightly modulated inducible NOS mRNA levels and endothelial NOS phosphorylation, whereas they were strongly increased after treatment with albumin-heme (Figure 3G and 3H). The upregulation of inducible NOS and the increased endothelial NOS phosphorylation
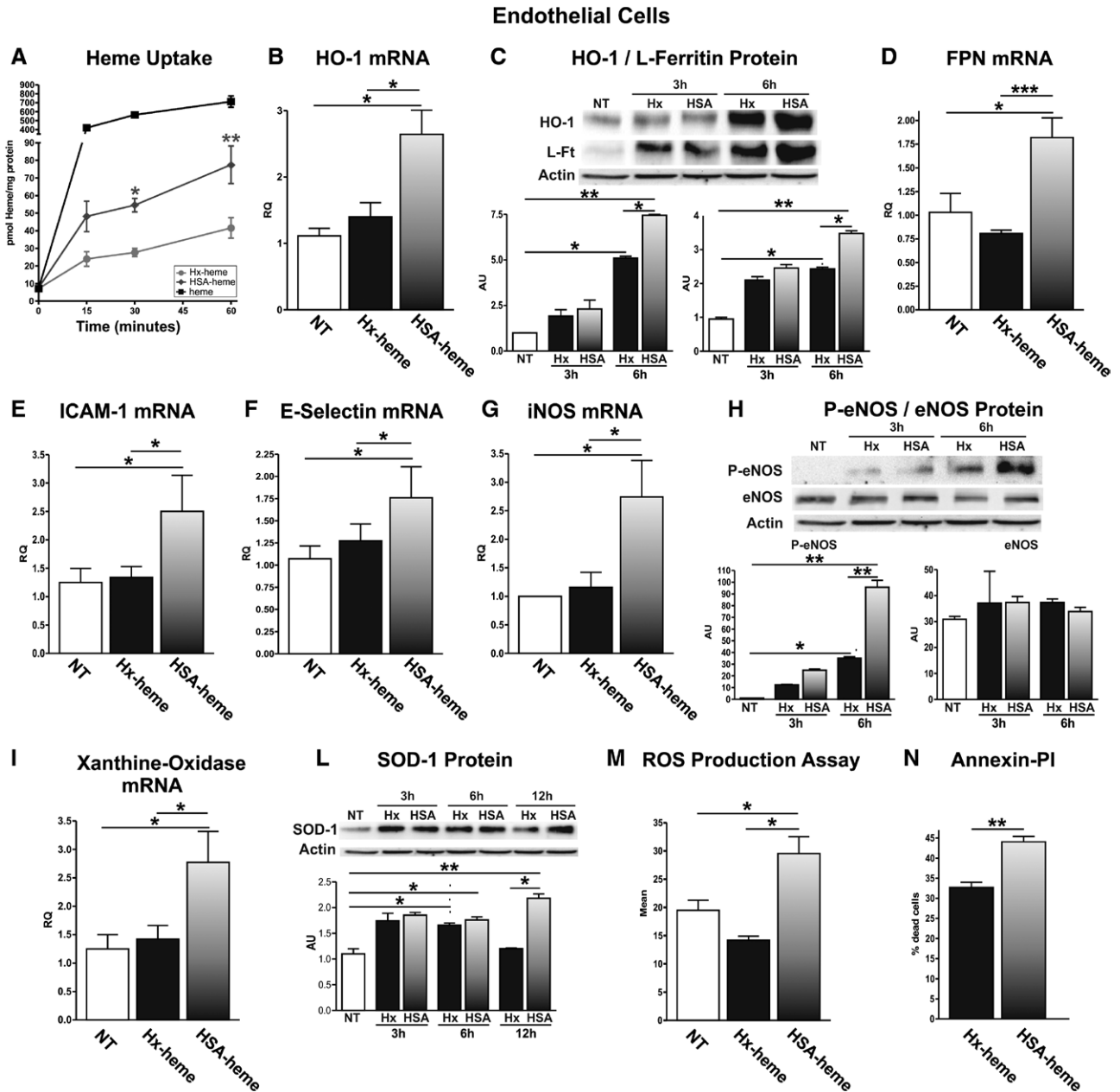
Endothelial Cells

Figure 3. Hemopexin (Hx) limits heme uptake by human umbilical vein endothelial cells (HUVECs). **A**, Heme uptake in HUVECs incubated with 7.5 µmol/L Hx-heme or human serum albumin (HSA)–heme for 15, 30, or 60 minutes (n=5). **B**, **D**, **E** through **G**, and **I**, Quantitative reverse transcription–polymerase chain reaction analysis of heme oxygenase-1 (HO-1), ferroportin (FPN), intercellular adhesion molecule-1 (ICAM-1), E-selectin, inducible nitric oxide synthase (iNOS), and xanthine oxidase mRNA levels in HUVECs incubated with 7.5 µmol/L Hx-heme or HSA-heme for 4 hours (n=6). **C**, **H**, and **L**, Representative Western blots of HO-1 and L-ferritin expression, phosphorylated endothelial nitric oxide synthase (P-eNOS) and eNOS expression, and superoxide dismutase 1 (SOD1) expression in HUVECs incubated with 7.5 µmol/L Hx-heme or HSA-heme for 4 hours (n=3). **M** and **N**, Representative fluorescence-activated cell sorted analysis of H_2DCFDA fluorescence and annexin V/propidium iodide (PI) staining in HUVECs treated with 10 µmol/L Hx-heme or HSA-heme for 20 hours (n=5). Values represent mean±SEM. Results shown are representative of 3 independent experiments. NT indicates not treated. *$P<0.05$; **$P<0.01$; ***$P<0.001$.

in albumin-heme treated cells plausibly occur as an attempt to compensate for the reduced NOS activity and increased NO oxidative consumption, as described above in aorta from heme-loaded Hx-null mice. In contrast to albumin, Hx strongly suppressed heme-induced ROS generation and oxidative stress in HUVECs (Figure 3I–3M). As a result, Hx limited heme-induced endothelial cell death (Figure 3N).

Taken together, these data confirmed the in vivo results and further proved that Hx prevents endothelial heme overload.

Similarly, Hx limited heme uptake by vascular smooth muscle cells in vitro (not shown).

Hx Prevents Endothelial Heme Loading and Toxicity by Promoting Hepatic Heme Detoxification

Data reported in the previous paragraph suggest that Hx may very efficiently counteract heme loading and toxicity on the vascular endothelium. To address the specific mechanism through which heme is inactivated after Hx binding,

we analyzed heme-overloaded Hx-null mice and found that these animals had a defect in hepatic heme accumulation and catabolism. As shown in Figure 4A and 4B, heme loading in the liver and in isolated hepatocytes was strongly reduced in heme-overloaded Hx-null mice compared with wild-type controls. Measurement of heme uptake on primary hepatocytes confirmed that heme entered very efficiently into these cells if bound to Hx but not if bound to albumin (Figure 4C).

Consistently, HO-1 protein was induced to a significantly lower extent in the liver of heme-overloaded Hx-null mice than in the liver of wild-type animals, and this correlated with a lower HO activity and a reduced induction of H- and L-ferritin (Figure 4D–4F) indicating that after heme overload, Hx-null liver produced less carbon monoxide and biliverdin and accumulated less iron. This was further demonstrated by the reduced bilirubin excretion into the bile of heme-overloaded Hx-null mice compared with wild-type animals (Figure IIa in the online-only Data Supplement). Consistent with data on bilirubin excretion, heme-overloaded Hx-null mice excreted a lower amount of intact heme into the bile compared with wild-type animals (Figure IIb and IIc in the online-only Data Supplement; additional data on hepatic heme metabolism in both the Results section and Figures I–III in the online-only Data Supplement).

Together, these data indicate that the lack of Hx in serum significantly affects the liver heme detoxifying potential and explain why in these conditions heme excess remains in the bloodstream, thus causing endothelial cell damage.

Hx Therapy Suppresses Heme-Driven Endothelial Activation in β-Thalassemic and SCD Mice

Data shown in the previous sections clearly linked vascular dysfunction to heme overload not buffered by plasma Hx. Because we observed that thalassemic and SCD mice experienced a condition of vascular damage associated with heme overload and Hx consumption (Figure 1), we hypothesized that an Hx-based therapy might be beneficial in hemolytic pathologies to limit endothelial dysfunction by increasing hepatic heme detoxifying potential.

To test this hypothesis, we treated 1-month-old thalassemic and SCD mice with 700 µg purified human Hx twice a week for 1 month, and at the end of the treatment, we analyzed the aortic endothelium. In Hx-treated thalassemic and SCD mice, we observed that iron accumulation was strongly reduced in the aortic endothelium and in the heart (Figure 5A and 5B), thus demonstrating that the exogenous Hx reduced endothelial heme loading in these mouse models of hemolysis. Accordingly, HO-1 was not induced in aortas of Hx-treated anemic mice, which correlated with an attenuated oxidative stress and with the reduced induction of adhesion molecules both in large vessels and in tissue vasculature (Figure 5C–5E).

Endothelial NOS mRNA level and NOS activity were increased whereas nitrotyrosine formation was strongly suppressed in aorta
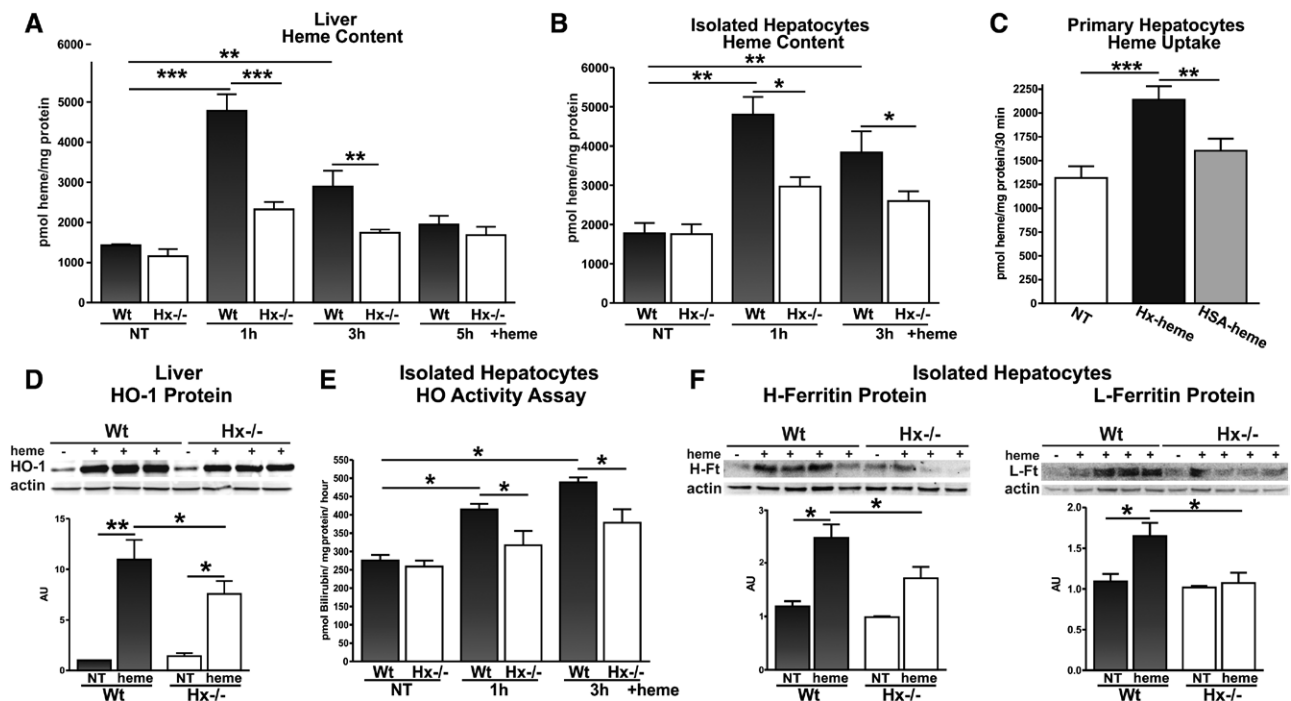
Figure 4. Hemopexin (Hx) promotes heme uptake and detoxification by the liver. **A**, Heme content in liver of wild-type (Wt) and Hx-null mice at different time points after heme injection (not treated [NT], n=4; 1 hour, n=3; 3 hours, n=6; 5 hours, n=5; liver: Hx–/–NT vs +heme, *P<0.05). **B**, Heme content in hepatocytes isolated from heme-overloaded Wt and Hx-null mice 1 and 3 hours after heme injection (NT, n=3; 1 hour, n=6; 3 hours, n=7). **C**, Heme content in primary hepatocytes treated with 5 µmol/L Hx-heme or human serum albumin (HSA)–heme in a 1:1 ratio for 30 minutes (n=11). **D**, Representative Western blot showing heme oxygenase-1 (HO-1) expression in total liver extracts from Wt and Hx-null mice 6 hours after heme injection (NT, n=3; heme, n=6). **E**, HO activity in hepatocytes isolated from Wt and Hx-null mice 1 and 3 hours after heme injection (n=4). **F**, Representative Western blots showing H- and L-ferritin expression in isolated hepatocyte extracts from Wt and Hx-null mice 6 hours after heme injection (NT, n=3; heme, n=6). Values represent mean±SEM. *P<0.05; **P<0.01; ***P<0.001.
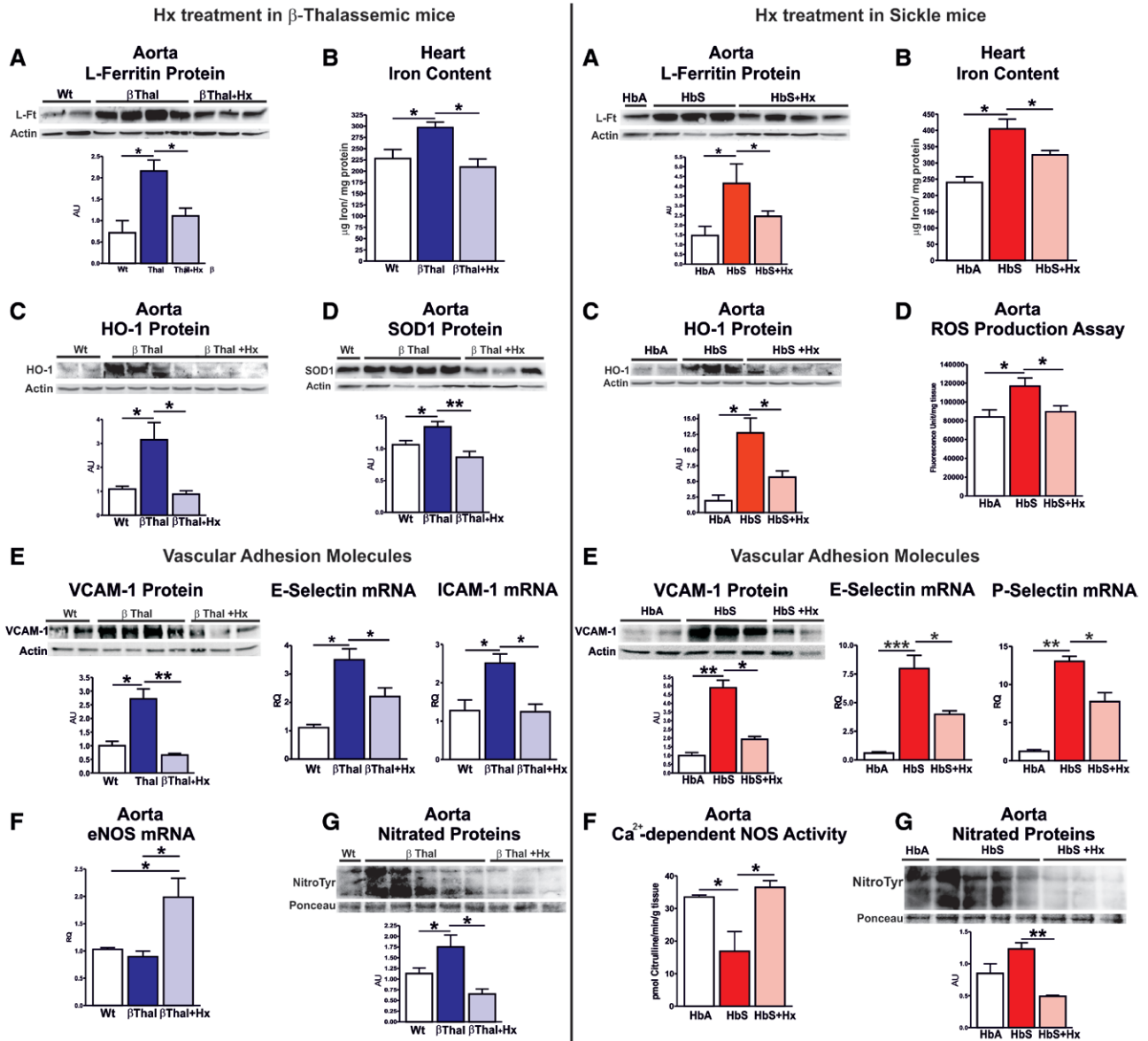
Figure 5. Hemopexin (Hx) therapy suppresses heme-driven endothelial activation in β-thalassemic (β-Thal) and sickle cell disease (SCD) mice. Data on wild-type (Wt), β-Thal, and Hx-treated β-Thal mice and normal hemoglobin (HbA), sickle hemoglobin (HbS), and Hx-treated HbS mice are shown on the **left** and **right**, respectively. **A**, Representative Western blot analysis of L-ferritin expression in aorta. **B**, Heart iron content. **C**, Representative Western blot showing heme oxygenase-1 (HO-1) expression in aorta. **D**, Representative Western blot showing superoxide dismutase 1 (SOD1) expression (**left**) and reactive oxygen species (ROS) production (**right**) in aorta. **E**, Representative Western blot showing vascular cell adhesion molecule-1 (VCAM-1) expression in aorta and quantitative reverse transcription–polymerase chain reaction (qRT-PCR) analysis of E-selectin and intercellular adhesion molecule-1 (ICAM-1)/P-selectin mRNA levels in liver. **F**, qRT-PCR analysis of endothelial nitric oxide synthase (eNOS) mRNA level (**left**) or calcium-dependent NOS activity (**right**) in extracts of aorta (n=4). Calcium-dependent NOS activity assay measures the activity of both inducible NOS (iNOS; calcium independent) and eNOS (calcium dependent), with eNOS being the most abundant NOS expressed in aorta. **G**, Representative Western blot showing nitrotyrosine formation in extracts of aorta. n=4. Values represent mean±SEM. Results shown are representative of 3 independent experiments. *P<0.05; **P<0.01; ***P<0.001.

of Hx-treated animals compared with untreated ones (Figure 5F and 5G), thus suggesting an increased availability of bioactive NO after Hx treatment. Similar to what occurs in large vessels, NOS activity was strongly suppressed in the liver of untreated animals and restored to normal levels after Hx administration, indicating that the whole vasculature was positively affected by Hx therapy (Results and Figure IV in the online-only Data Supplement). The same parameters were analyzed in Hx-treated wild-type and HbA mice, and no significant effect of exogenous Hx was detected in these animals (not shown).

Thus, Hx administration successfully alleviates heme-induced endothelial alterations in thalassemic and SCD mice.

Hx-Mediated Endothelial Protection in β-Thalassemic and SCD Mice Is Due to an Enhanced Hepatic Heme Detoxification

We asked whether the Hx protective effect on the endothelium of thalassemic and SCD mice was due specifically to the enhancement of their hepatic heme detoxifying potential mediated by exogenous Hx.

Analysis of heme-overloaded Hx-null mice demonstrated that exogenous human Hx was able to fully rescue their hepatic heme recovery capacity (Results and Figure V in the online-only Data Supplement). In Hx-treated thalassemic and SCD mice, we observed that iron accumulated in a significantly higher amount in the liver compared with untreated animals (Figure 6A). In these animals, Hx administration consistently reduced the amount of circulating heme (not shown) and total bilirubin (Figure VIa in the online-only Data Supplement) while enhancing HO-1 mRNA levels in the liver (Figure 6B), as well as bilirubin and heme excretion in the bile (Figure VIb and VIc in the online-only Data Supplement).

Together, these data demonstrated that Hx therapy enhanced liver detoxifying potential and restored iron homeostasis in thalassemic and SCD mice. This was associated with an attenuated oxidative stress, improved control of the inflammatory response, and amelioration of the liver status (Figure 6C–6F). On the other hand, we did not observe changes in red cell indexes in Hx-treated mice from both mouse strains compared with baseline values (Table II in the online-only Data Supplement).

Hx Therapy Normalizes Blood Pressure and Improves Cardiac Function in SCD Mice

Our results in anemic mice showing enhanced endothelial activation and reduced NO bioavailability support the idea that these animals could have altered cardiovascular function. It has consistently been reported recently that 10- to 14-month-old thalassemic mice show left ventricular hypertrophy and decreased fractional shortening and ejection fraction.[34] Because our data on endothelium (Figure 5) indicated that the damage was worse in SCD mice, we supposed that cardiac function might become altered earlier in these animals. Indeed, measurement of blood pressure and echocardiography analysis on 2-month-old SCD mice demonstrated that HbS mice were hypertensive compared with HbA controls, showing a 1.6-fold increase in mean arterial blood pressure (Figure VIIa in the online-only Data Supplement). An enhancement of both systolic and diastolic pressures contributed to an increase in mean arterial blood pressure, as shown in Figure VIIb in the online-only Data Supplement. Moreover, SCD mice showed increased cardiac output and aortic valve peak pressure that were 2.8- and 4.5-fold higher, respectively,
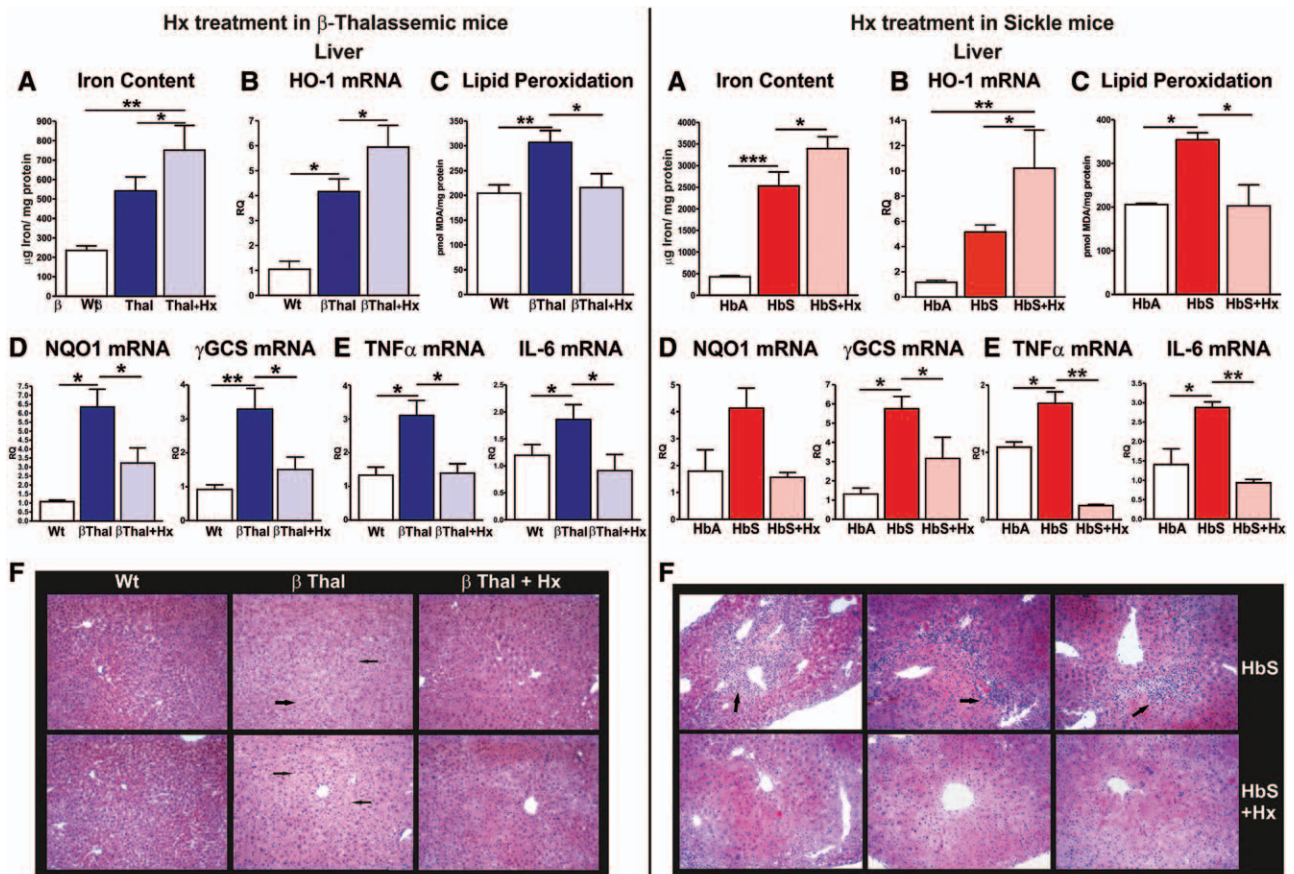
Figure 6. Hemopexin (Hx) therapy promotes hepatic heme detoxification in β-thalassemic (β-Thal) and sickle cell disease (SCD) mice. Data on wild-type (Wt), β-Thal, and Hx-treated β-Thal mice and normal hemoglobin (HbA), sickle hemoglobin (HbS), and Hx-treated HbS mice are shown on the **left** and **right**, respectively. **A**, Iron content and (**B**) quantitative reverse transcription–polymerase chain reaction (qRT-PCR) analysis of heme oxygenase-1 (HO-1) mRNA level in liver. **C**, Liver malondialdehyde content. **D**, qRT-PCR analysis of NAD(P)H dehydrogenase, quinone 1 and γ-Glutamylcysteine synthetase mRNA levels and (**E**) of tumor necrosis factor-α (TNFα) and interleukin-6 (IL-6) mRNA levels in liver. n=4. Values represent mean±SEM. Results shown are representative of 3 independent experiments. *P<0.05; **P<0.01; ***P<0.001. **F**, Representative liver sections stained with hematoxylin and eosin. Arrows indicate sites of cell necrosis (**left**), evident in β-Thal mice but not in Hx-treated animals, and leukocyte aggregates (**right**), the number of which was strongly reduced by Hx administration in SCD mice.

compared with HbA mice (Figure VIIc and VIId and Table III in the online-only Data Supplement). Increased blood pressure and cardiac output[35] were found to be associated with an increased hypertrophic response and a significant reduction in myocardial performance[36] (Table III in the online-only Data Supplement).

Because we demonstrated that Hx therapy decreased ROS production and NO oxidative consumption in the vascular endothelium of SCD mice, we hypothesized that Hx administration might positively affect cardiovascular function in these animals. To test this hypothesis, we monitored blood pressure in Hx-treated HbS mice during the therapy. Blood pressure was significantly reduced by Hx treatment starting from the first administration and almost completely normalized by the fourth injection (Figure 7A). A reduction in both systolic and diastolic pressures accounted for blood pressure normalization (Figure 7B). This potent antihypertensive effect of Hx was further confirmed on 5-month-old HbS mice, which showed a full rescue in mean arterial blood pressure after a single 3-mg Hx injection (Figure 7C). Accordingly, cardiac output and aortic valve peak pressure were restored to normal values by Hx treatment (Figure 7D–7F and Figure VIII and Table III in the online-only Data Supplement). As a result, the performance index of the left ventricle was improved in Hx-treated HbS mice (Figure 7G).

These data highlight the critical importance of Hx in preventing heme-mediated vascular oxidative stress and in rescuing cardiovascular function in a mouse model of SCD.

Discussion

Here, we showed that Hx infusion alleviates heme-induced endothelial activation and maintains vascular homeostasis in 2 mouse models of β-thalassemia and SCD, thus suggesting important implications for the therapeutic use of Hx to treat vasculopathy in hemolytic disorders. Moreover, we reported that in SCD mice vascular damage was associated with altered cardiac function, which was restored by Hx therapy. These data demonstrate that heme has a strong impact on cardiovascular function and highlight the efficacy of a therapy specifically aimed at chelating free heme.
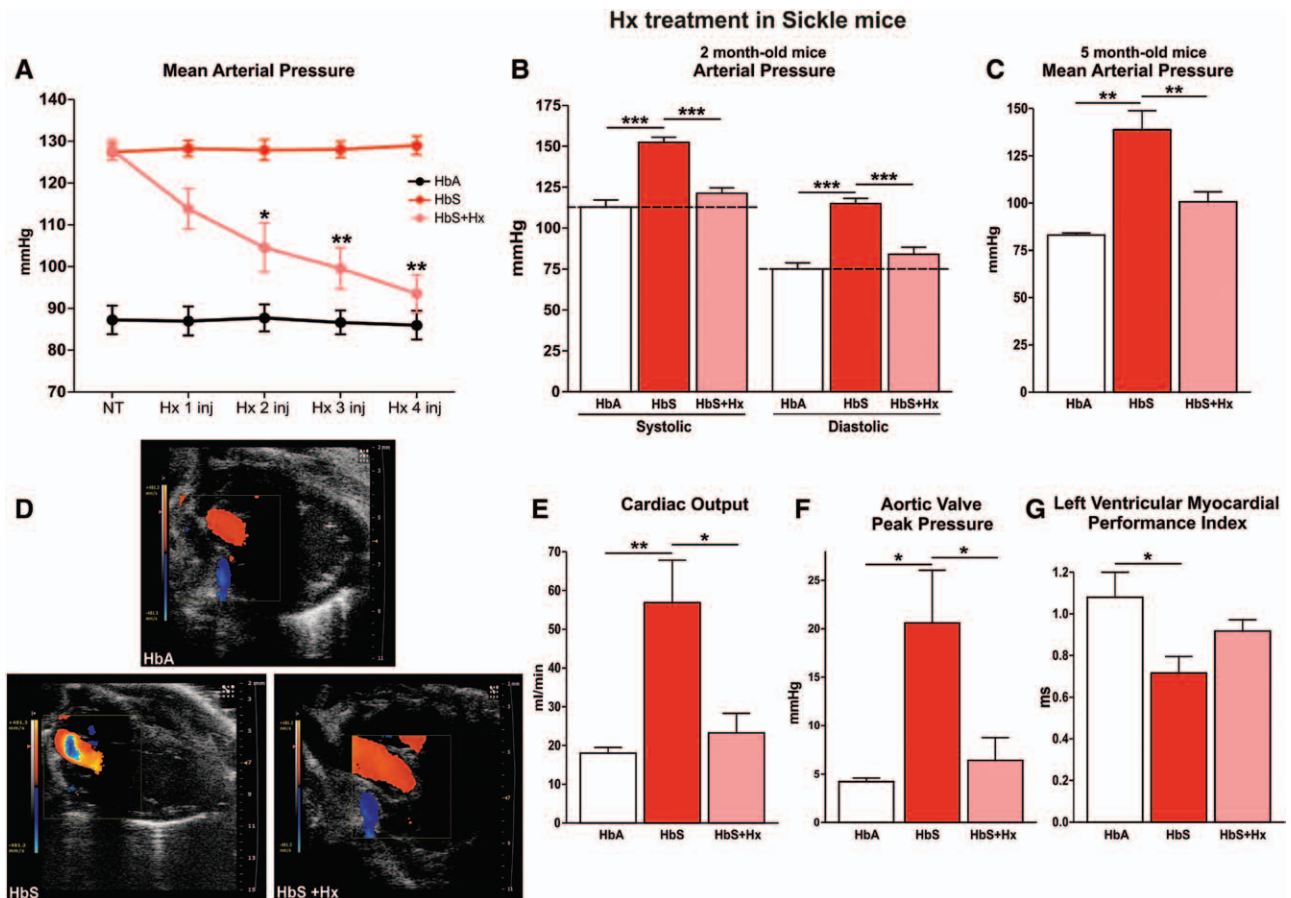
Figure 7. Hemopexin (Hx) administration normalizes blood pressure and improves cardiac function in sickle cell disease (SCD) mice. **A**, Mean arterial pressure in 1-month-old normal hemoglobin (HbA), sickle hemoglobin (HbS), and Hx-treated HbS mice measured before and during treatment (0.7 mg Hx in each injection; n=5). HbA vs HbS: ***$P<0.001$ at each point. **B**, Systolic and diastolic pressures measured after the fourth Hx injection (n=5). **C**, Mean arterial pressure in 5-month-old HbA, HbS, and Hx-treated HbS mice (a single 3-mg Hx dose; n=4). **D**, Representative images of color Doppler on the left ventricular outflow tract (LVOT) in HbA, HbS, and Hx-treated HbS mice. **E** through **G**, Cardiac output, aortic valve peak pressure, and left ventricular myocardial performance index measured in HbA, HbS, and Hx-treated HbS mice by echocardiography (n=6). Values represent mean±SEM. Results shown are representative of 3 independent experiments. *$P<0.05$; **$P<0.01$; ***$P<0.001$.

Hx exerts its protective effect mainly by promoting heme recovery and detoxification through HO activity in the liver and by limiting heme-iron loading and HO-1 induction[37] in the vascular endothelium. Patients and mice suffering from SCD showed an adaptive upregulation of HO-1 in response to hemolysis, which often was insufficient to completely handle the excessive heme burden, particularly during acute bouts of hemolysis.[9] Hx therapy demonstrates that a major benefit is obtained by HO activity induction in hepatocytes, likely because the liver is well equipped to manage high amounts of heme. The enhanced heme-iron accumulation in the liver of Hx-treated anemic mice resulted in a strong increase in hepatic heme detoxifying potential and in the protection of nonhepatic tissues from heme accumulation and its toxic effects.[38] Indeed, an important outcome of Hx therapy is the prevention of heme-iron loading in the vascular endothelium and in the heart. This is clinically relevant because hemolysis-driven iron overload, further exacerbated by transfusion regimen, strongly contributes to heart failure in β-thalassemia patients, representing the most common cause of death in these subjects.[39]

The critical role of heme-driven endothelial activation in the pathophysiology of β-thalassemia and SCD has been recently recognized, and its contribution to vascular instability and vaso-occlusive events has been described.[5,9,40,41] Because of chronic hemolysis, vessels of thalassemic and SCD patients are exposed to great amounts of ROS catalyzed by heme-derived redox-active iron[1,5,6,8] that lead to endothelial activation and adhesion molecule expression on the vessel wall, which in turn favors the adhesion of red blood cells and leukocytes, resulting in vascular instability and vaso-occlusion.[9,40–42] Serum heme overload properly correlates with the increased tissue oxidation and antioxidant response and with endothelial activation, inflammation, and plasma Hb/heme scavenger depletion.

Here, we demonstrated that Hx administration, by scavenging free heme, alleviates heme-induced tissue oxidative injury and limits the induction of adhesion molecules, the formation of ROS in the vascular endothelium, and the production of proinflammatory cytokines in both β-thalassemia and SCD mouse models. This indicates that Hx may confer protection against heme-driven endothelial activation, oxidative stress, and inflammation.[43]

The vascular dysfunction common to both β-thalassemia and SCD is further amplified by the reduced bioavailability of NO as major vasodilator, resulting in imbalance of vascular tone toward vasoconstriction.[4,11,22,44,45] In β-thalassemia and SCD, consumption/inactivation of NO is accelerated by the synergistic effects of chronic oxidative stress and persistent hemolysis.[1,4] In these patients, increased ROS production is implicated in the NO consumption and formation of peroxynitrite (ONOO⁻) that resulted in nitrotyrosine formation.[46,47] NOS itself can be uncoupled by oxidation of the essential cofactor BH4, and uncoupled NOS produces superoxide in place of NO.[1] Excessive peroxynitrite formation further contributes to NOS activity reduction and NOS dimer disruption. Consistently, elevated nitrotyrosine levels correlate with impaired NOS activity and loss of NOS dimerization in SCD mice.[35] Furthermore, NO is rapidly destroyed by its reaction to the iron contained in free heme/Hb present in the plasma.[1] Hemolysis also releases red cell arginase-1 into plasma, thus reducing the levels of NOS substrate and L-arginine and further limiting NO bioavailability.[1,4,11] As a result, in these pathological conditions, vascular endothelium is likely to be in a perpetually activated state because of chronic oxidative stress and reduced NO consequent to hemolysis. Agents directed at restoring NO homeostasis could be promising to alleviate vascular instability in patients suffering from β-thalassemia and SCD. Here, we observed enhanced NOS activity in the vascular endothelium of Hx-treated thalassemic and SCD mice, suggesting that Hx could promote NO production by reducing the oxidative consumption of NOS cofactors and NOS uncoupling. Moreover, Hx treatment reduced nitrotyrosine formation, a footprint of NO-ROS interaction and peroxynitrite production, in both mouse models of β-thalassemia and SCD. Together, these results demonstrate that, after Hx administration, more NO is produced and less NO is oxidatively inactivated in the endothelium, resulting in an increased availability of bioactive NO, which could be beneficial for counteracting the endothelial dysfunction associated with these hemolytic pathologies.

We found that in SCD mice, oxidative stress and reduced NO availability are associated with systemic hypertension, and Hx therapy, by restoring normal NO levels and reducing ROS production, normalizes blood pressure. This strong antihypertensive effect of Hx suggests the possibility of using Hx-based drugs to counteract the systemic vasoconstriction promoted by free heme.

Although traditionally associated with systemic vasoconstriction, endothelial dysfunction was recently proposed to play a central role even in heart failure pathogenesis. The failing heart is characterized by an altered redox state with ROS overproduction, and increasing evidence suggests that the abnormal cardiac and vascular phenotypes characterizing the failing heart are caused in large part by imbalances between NO bioavailability and oxidative stress.[48] Our results are consistent with these findings in that we showed that low NO and high ROS in SCD mice were associated with impaired cardiac performance. Our data strengthen the central role of heme in triggering these processes. Taking into account that heme is released not only during hemolysis associated with hemoglobinopathies but also after ischemia/reperfusion injury and cardiac remodeling, these observations could be of a broader importance.

The administration of antioxidants,[49,50] endothelial activation inhibitors,[51] or NO donors[52,53] has been shown to positively affect vascular function in hemolytic diseases. In this scenario, Hx therapy could contribute to restoration of cardiovascular homeostasis, targeting multiple steps involved in the pathogenesis of vasculopathy and consequent cardiac decay. Indeed, we showed that in SCD mice Hx treatment not only beneficially affected the imbalance between vasodilator/vasoconstrictor factors but also significantly improved cardiac performance.
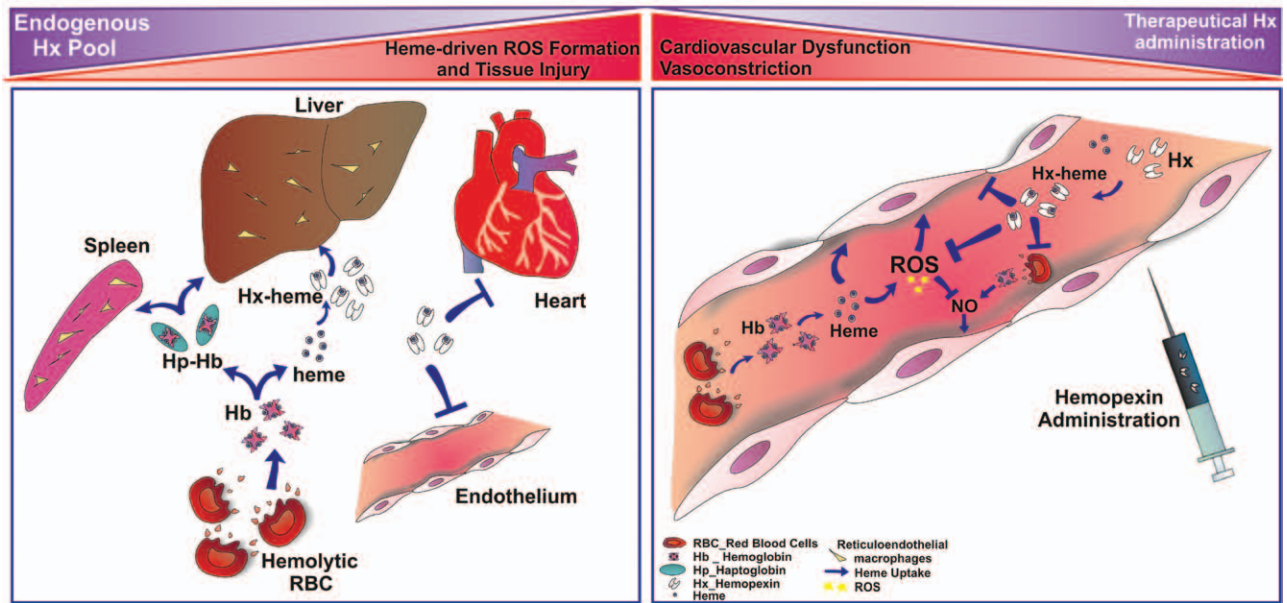
Figure 8. Proposed mechanism for hemopexin (Hx) action. Hx acts as a heme chelator that promotes heme uptake and detoxification by liver (**left**). In hemolytic diseases, the exhaustion of the Hx plasma pool leads to a significant reduction of the hepatic heme detoxifying potential and finally to heme recovery by vascular endothelial cells and heart. In this condition, heme directly acts on the endothelial wall, causing oxidative damage; it intercalates into red blood cell (RBC) membrane, amplifying hemolysis and hemoglobin (Hb) release, and strongly enhances reactive oxygen species (ROS) production. All these mechanisms contribute to oxidative damage, nitric oxide depletion, and endothelial activation, thus altering vascular homeostasis. Hx administration in hemolytic pathologies, by scavenging free heme, blocks heme toxic effects and improves cardiovascular function (**right**).

Consistent with our results on SCD mice, others have recently reported that even thalassemic mice developed cardiovascular dysfunction with aging,[34,45] thus suggesting that the deterioration of cardiovascular function may occur more slowly in these animals. This is consistent with our data showing milder endothelial damage in thalassemic compared with SCD mice and further strengthens the relationship between endothelial dysfunction and heart damage. From the observation that heme overload had similar toxic effects on the endothelium of both mouse models, it is likely that a long-term Hx therapy also might beneficially affect cardiovascular function in β-thalassemia.

Conclusions

We propose a pivotal role for Hx as a potent free heme scavenger to treat vasculopathy related to hemolytic disorders. In fact, Hx avoids heme intercalation in cell membranes, thus limiting lipid peroxidation, cell oxidative stress, and hemolysis amplification. Moreover, Hx prevents free heme-mediated generation of ROS that directly act on the endothelial wall and inactivate NO, thus impairing vascular function (Figure 8). The final outcome of the Hx therapy is the preservation of cardiovascular function.

Thus, purified or recombinant Hx might be used pharmacologically for the treatment of patients with hemolytic diseases. Because Hx acts as a heme chelator, it could be used with iron chelators,[28] the administration of which is usually associated with blood transfusion[25,26] in anemic patients, as a specific therapy to counteract heme toxicity, thus enhancing the effectiveness of the chelation therapy and preserving cardiovascular function.

References

1. Morris CR. Mechanisms of vasculopathy in sickle cell disease and thalassemia. *Hematology Am Soc Hematol Educ Program*. 2008:177–185.
2. Rother RP, Bell L, Hillmen P, Gladwin MT. The clinical sequelae of intravascular hemolysis and extracellular plasma hemoglobin: a novel mechanism of human disease. *JAMA*. 2005;293:1653–1662.
3. Olivieri NF. The beta-thalassemias. *N Engl J Med*. 1999;341:99–109.
4. Abboud MR, Musallam KM. Sickle cell disease at the dawn of the molecular era. *Hemoglobin*. 2009;33 Suppl 1:S93–S106.
5. Belcher JD, Bryant CJ, Nguyen J, Bowlin PR, Kielbik MC, Bischof JC, Hebbel RP, Vercellotti GM. Transgenic sickle mice have vascular inflammation. *Blood*. 2003;101:3953–3959.

6. Wagener FA, Abraham NG, van Kooyk Y, de Witte T, Figdor CG. Heme-induced cell adhesion in the pathogenesis of sickle-cell disease and inflammation. *Trends Pharmacol Sci*. 2001;22:52–54.

7. Balla J, Vercellotti GM, Jeney V, Yachie A, Varga Z, Eaton JW, Balla G. Heme, heme oxygenase and ferritin in vascular endothelial cell injury. *Mol Nutr Food Res*. 2005;49:1030–1043.

8. Jeney V, Balla J, Yachie A, Varga Z, Vercellotti GM, Eaton JW, Balla G. Pro-oxidant and cytotoxic effects of circulating heme. *Blood*. 2002;100:879–887.

9. Belcher JD, Beckman JD, Balla G, Balla J, Vercellotti G. Heme degradation and vascular injury. *Antioxid Redox Signal*. 2010;12: 233–248.

10. Kumar S, Bandyopadhyay U. Free heme toxicity and its detoxification systems in human. *Toxicol Lett*. 2005;157:175–188.

11. Wood KC, Hsu LL, Gladwin MT. Sickle cell disease vasculopathy: a state of nitric oxide resistance. *Free Radic Biol Med*. 2008;44:1506–1528.

12. Gozzelino R, Jeney V, Soares MP. Mechanisms of cell protection by heme oxygenase-1. *Annu Rev Pharmacol Toxicol*. 2010;50:323–354.

13. Kovtunovych G, Eckhaus MA, Ghosh MC, Ollivierre-Wilson H, Rouault TA. Dysfunction of the heme recycling system in heme oxygenase 1-deficient mice: effects on macrophage viability and tissue iron distribution. *Blood*. 2010;116:6054–6062.

14. Tolosano E, Fagoone S, Morello N, Vinchi F, Fiorito V. Heme scavenging and the other facets of hemopexin. *Antioxid Redox Signal*. 2010;12:305–320.

15. Tenhunen R, Marver HS, Schmid R. The enzymatic conversion of heme to bilirubin by microsomal heme oxygenase. *Proc Natl Acad Sci U S A*. 1968;61:748–755.

16. Wagener FA, Volk HD, Willis D, Abraham NG, Soares MP, Adema GJ, Figdor CG. Different faces of the heme-heme oxygenase system in inflammation. *Pharmacol Rev*. 2003;55:551–571.

17. Muller-Eberhard U, Javid J, Liem HH, Hanstein A, Hanna M. Plasma concentrations of hemopexin, haptoglobin and heme in patients with various hemolytic diseases. *Blood*. 1968;32:811–815.

18. Hebbel RP, Vercellotti G, Nath KA. A systems biology consideration of the vasculopathy of sickle cell anemia: the need for multi-modality chemo-prophylaxis. *Cardiovasc Hematol Disord Drug Targets*. 2009;9: 271–292.

19. Aslan M, Freeman BA. Redox-dependent impairment of vascular function in sickle cell disease. *Free Radic Biol Med*. 2007;43:1469–1483.

20. Ataga KI, Cappellini MD, Rachmilewitz EA. Beta-thalassaemia and sickle cell anaemia as paradigms of hypercoagulability. *Br J Haematol*. 2007;139:3–13.

21. Detchaporn P, Kukongviriyapan U, Prawan A, Jetsrisuparb A, Greenwald SE, Kukongviriyapan V. Altered vascular function, arterial stiffness, and antioxidant gene responses in pediatric thalassemia patients. *Pediatr Cardiol*. 2012;33:1054–1060.

22. Hahalis G, Kremastinos DT, Terzis G, Kalogeropoulos AP, Chrysanthopoulou A, Karakantza M, Kourakli A, Adamopoulos S, Tselepis AD, Grapsas N, Siablis D, Zoumbos NC, Alexopoulos D. Global vasomotor dysfunction and accelerated vascular aging in beta-thalassemia major. *Atherosclerosis*. 2008;198:448–457.

23. Frenette PS, Atweh GF. Sickle cell disease: old discoveries, new concepts, and future promise. *J Clin Invest*. 2007;117:850–858.

24. De Franceschi L, Bertoldi M, De Falco L, Santos Franco S, Ronzoni L, Turrini F, Colancecco A, Camaschella C, Cappellini MD, Iolascon A. Oxidative stress modulates heme synthesis and induces peroxiredoxin-2 as a novel cytoprotective response in β-thalassemic erythropoiesis. *Haematologica*. 2011;96:1595–1604.

25. Perrotta PL, Snyder EL. Non-infectious complications of transfusion therapy. *Blood Rev*. 2001;15:69–83.

26. Wahl S, Quirolo KC. Current issues in blood transfusion for sickle cell disease. *Curr Opin Pediatr*. 2009;21:15–21.

27. Aggeli C, Antoniades C, Cosma C, Chrysohoou C, Tousoulis D, Ladis V, Karageorga M, Pitsavos C, Stefanadis C. Endothelial dysfunction and inflammatory process in transfusion-dependent patients with beta-thalassemia major. *Int J Cardiol*. 2005;105:80–84.

28. Brittenham GM. Iron-chelating therapy for transfusional iron overload. *N Engl J Med*. 2011;364:146–156.

29. Vinchi F, Gastaldi S, Silengo L, Altruda F, Tolosano E. Hemopexin prevents endothelial damage and liver congestion in a mouse model of heme overload. *Am J Pathol*. 2008;173:289–299.

30. Ryan TM, Ciavatta DJ, Townes TM. Knockout-transgenic mouse model of sickle cell disease. *Science*. 1997;278:873–876.

31. Wu LC, Sun CW, Ryan TM, Pawlik KM, Ren J, Townes TM. Correction of sickle cell disease by homologous recombination in embryonic stem cells. *Blood*. 2006;108:1183–1188.

32. De Franceschi L, Daraio F, Filippini A, Carturan S, Muchitsch EM, Roetto A, Camaschella C. Liver expression of hepcidin and other iron genes in two mouse models of beta-thalassemia. *Haematologica*. 2006;91:1336–1342.

33. Tolosano E, Hirsch E, Patrucco E, Camaschella C, Navone R, Silengo L, Altruda F. Defective recovery and severe renal damage after acute hemolysis in hemopexin-deficient mice. *Blood*. 1999;94:3906–3914.

34. Stoyanova E, Cloutier G, Felfly H, Lemsaddek W, Ah-Son N, Trudel M. Evidence for a novel mechanism independent of myocardial iron in β-thalassemia cardiac pathogenesis. *PLoS ONE*. 2012;7:e52128.

35. Hsu LL, Champion HC, Campbell-Lee SA, Bivalacqua TJ, Manci EA, Diwan BA, Schimel DM, Cochard AE, Wang X, Schechter AN, Noguchi CT, Gladwin MT. Hemolysis in sickle cell mice causes pulmonary hypertension due to global impairment in nitric oxide bioavailability. *Blood*. 2007;109:3088–3098.

36. Voskaridou E, Christoulas D, Terpos E. Sickle-cell disease and the heart: review of the current literature. *Br J Haematol*. 2012;157:664–673.

37. Paine A, Eiz-Vesper B, Blasczyk R, Immenschuh S. Signaling to heme oxygenase-1 and its anti-inflammatory therapeutic potential. *Biochem Pharmacol*. 2010;80:1895–1903.

38. Smith A, Morgan WT. Transport of heme by hemopexin to the liver: evidence for receptor-mediated uptake. *Biochem Biophys Res Commun*. 1978;84:151–157.

39. Wood JC, Tyszka JM, Carson S, Nelson MD, Coates TD. Myocardial iron loading in transfusion-dependent thalassemia and sickle cell disease. *Blood*. 2004;103:1934–1936.

40. Belcher JD, Mahaseth H, Welch TE, Vilback AE, Sonbol KM, Kalambur VS, Bowlin PR, Bischof JC, Hebbel RP, Vercellotti GM. Critical role of endothelial cell activation in hypoxia-induced vasoocclusion in transgenic sickle mice. *Am J Physiol Heart Circ Physiol*. 2005;288:H2715–H2725.

41. Belcher JD, Mahaseth H, Welch TE, Otterbein LE, Hebbel RP, Vercellotti GM. Heme oxygenase-1 is a modulator of inflammation and vaso-occlusion in transgenic sickle mice. *J Clin Invest*. 2006;116:808–816.

42. Belcher JD, Marker PH, Weber JP, Hebbel RP, Vercellotti GM. Activated monocytes in sickle cell disease: potential role in the activation of vascular endothelium and vaso-occlusion. *Blood*. 2000;96:2451–2459.

43. Fink MP. Editorial: hemopexin: newest member of the anti-inflammatory mediator club. *J Leukoc Biol*. 2009;86:203–204.

44. Siciliano A, Malpeli G, Platt OS, Lebouef C, Janin A, Scarpa A, Olivieri O, Amato E, Corrocher R, Beuzard Y, De Franceschi L. Abnormal modulation of cell protective systems in response to ischemic/reperfusion injury is important in the development of mouse sickle cell hepatopathy. *Haematologica*. 2011;96:24–32.

45. Stoyanova E, Trudel M, Felfly H, Lemsaddek W, Garcia D, Cloutier G. Vascular endothelial dysfunction in β-thalassemia occurs despite increased eNOS expression and preserved vascular smooth muscle cell reactivity to NO. *PLoS ONE*. 2012;7:e38089.

46. Aslan M, Ryan TM, Adler B, Townes TM, Parks DA, Thompson JA, Tousson A, Gladwin MT, Patel RP, Tarpey MM, Batinic-Haberle I, White CR, Freeman BA. Oxygen radical inhibition of nitric oxide-dependent vascular function in sickle cell disease. *Proc Natl Acad Sci U S A*. 2001;98:15215–15220.

47. Kaul DK, Liu XD, Chang HY, Nagel RL, Fabry ME. Effect of fetal hemoglobin on microvascular regulation in sickle transgenic-knockout mice. *J Clin Invest*. 2004;114:1136–1145.

48. Marti CN, Gheorghiade M, Kalogeropoulos AP, Georgiopoulou VV, Quyyumi AA, Butler J. Endothelial dysfunction, arterial stiffness, and heart failure. *J Am Coll Cardiol*. 2012;60:1455–1469.

49. Kaul DK, Liu XD, Zhang X, Ma L, Hsia CJ, Nagel RL. Inhibition of sickle red cell adhesion and vasoocclusion in the microcirculation by antioxidants. *Am J Physiol Heart Circ Physiol*. 2006;291:H167–H175.

50. Kaul DK, Zhang X, Dasgupta T, Fabry ME. Arginine therapy of transgenic-knockout sickle mice improves microvascular function by reducing non-nitric oxide vasodilators, hemolysis, and oxidative stress. *Am J Physiol Heart Circ Physiol*. 2008;295:H39–H47.

51. Hebbel RP, Vercellotti GM, Pace BS, Solovey AN, Kollander R, Abanonu CF, Nguyen J, Vineyard JV, Belcher JD, Abdulla F, Osifuye S, Eaton JW, Kelm RJ Jr, Slungaard A. The HDAC inhibitors trichostatin A and suberoylanilide hydroxamic acid exhibit multiple modalities of benefit for the vascular pathobiology of sickle transgenic mice. *Blood*. 2010;115:2483–2490.

52. de Franceschi L, Baron A, Scarpa A, Adrie C, Janin A, Barbi S, Kister J, Rouyer-Fessard P, Corrocher R, Leboulch P, Beuzard Y. Inhaled nitric oxide protects transgenic SAD mice from sickle cell disease-specific lung injury induced by hypoxia/reoxygenation. *Blood*. 2003;102:1087–1096.

53. de Franceschi L, Malpeli G, Scarpa A, Janin A, Muchitsch EM, Roncada P, Leboeuf C, Corrocher R, Beuzard Y, Brugnara C. Protective effects of S-nitrosoalbumin on lung injury induced by hypoxia-reoxygenation in mouse model of sickle cell disease. *Am J Physiol Lung Cell Mol Physiol*. 2006;291:L457–L465.

CLINICAL PERSPECTIVE

Two worldwide-distributed hemolytic anemias are sickle cell disease and β-thalassemia. Both disorders are characterized by inflammatory vasculopathy resulting from a complex scenario involving abnormal red cells, neutrophils, proinflammatory cytokines, and a highly pro-oxidant plasma environment. The destruction of abnormal red cells induced both intravascular and extravascular hemolysis. Intravascular hemolysis is characterized by the presence of an aliquot of plasma free hemoglobin that rapidly losses its heme group, binding the endogenous hemopexin (Hx). Thus, hemolytic anemias are characterized by relative Hx deficiency with the presence of circulating toxic free heme. This promotes membrane lipid peroxidation and severe cell oxidative stress with the production of reactive oxygen species that act directly on the endothelial wall and inactivate nitric oxide, impairing vascular function. Here, we show that treatment with exogenous Hx promotes heme recovery and prevents heme-iron loading in endothelial and heart cells, limiting the induction of heme oxygenase-1, adhesion molecules, reactive oxygen species production, and nitric oxide synthase/nitric oxide oxidative inactivation. In sickle cell disease mice, Hx reduced blood pressure and restored cardiac output, suggesting a key role for Hx in the protection against heme-induced cardiovascular dysfunction. We propose Hx as potent free-heme scavenger to be used as an additional therapeutic tool in the treatment of vasculopathy related to hemolytic disorders.

Hemopexin therapy improves cardiovascular function by preventing heme-induced endothelial toxicity in mouse models of hemolytic diseases

Francesca Vinchi[1,2] PhD, Lucia De Franceschi[3] MD, Alessandra Ghigo[1,2] PhD, Tim Townes[4] PhD, James Cimino[1,2] BSc, Lorenzo Silengo[1,2] MD, Emilio Hirsch[1,2] PhD, Fiorella Altruda[1,2] PhD, and Emanuela Tolosano[1,2] PhD

SUPPLEMENTAL MATERIAL

Supplemental Material and Methods

Mice and treatments

A mouse strain that underexpresses β-globin chains, the Hbb[th1/th1] mouse, was used as a model of β-thalassemia intermedia[1]. This mouse model has arisen as a spontaneous DNA deletion of the β major gene[2, 3]. Wild-type animals of the same genetic background were used as controls. As a model of SCD, a humanized knock-in mouse in which the murine α-globin and β-globin genes were replaced with human α-globin and with human Aγ and β[S] (sickle) globin genes respectively, was employed[2]. SCD mice (HbS) were compared to their counterpart carrying the human Aγ and β alleles in homozigosity (HbA).

Mice used in these studies were 2/3-month-old littermates, maintained on a standard chow diet and kept with free access to food and water. All experiments were approved by the animal ethical committee of the University of Torino (Italy).

Hemin and Tin-protoporphyrin IX (Frontier Scientific, Logan, Utah) were freshly prepared as previously reported[4], and injected into the tail vein of wild-type and Hx-null mice at a dose of 30μmol/kg. Control mice were injected with PBS. Mice were sacrificed at different times after hemin injection. Mice were anesthetized, tissue samples collected and kept frozen until analysis. Blood was collected by retro-orbital bleeding.

For rescue experiment, 1500μg of human Hx (Athens Research, GA, USA) were injected iv in Hx-null mice. After 1 hour, the same mice were subjected to heme injection and sacrificed 60 min later.

Primary Hepatocyte culture preparation

Hepatocytes were isolated from single hepatic lobules[5]. After liver dissection, the single liver lobe was perfused using Hepatocyte Liver Perfusion Medium and then Hepatocyte Liver Digest Medium (Gibco). Perfusion with Digest Medium was kept until the liver lobe felt very soft. This is a critical step, as this medium contains collagenase, and excessive digestion should be avoid to prevent cell death. Subsequently, the perfused liver lobe was disrupted and the cell suspension was forced through a 100 μm Cell Strainer (BD). Cells were centrifuged and then cell suspension was applied

over a Percoll gradient. After Percoll gradient centrifugation the two upper layers that contain cell debris and non-parenchymal cells were carefully pipetted out and discarded. Then, the lowest layer that contains the live hepatocytes was collected. Cells were washed, centrifuged and then plated onto collagen-coated well plates.

Heme Content Quantification

Heme content in tissues and in bile samples was quantified fluorometrically by the method of Sassa[6]. Briefly, tissues were homogenized in phosphate buffer saline (PBS) and protein content was determined by using the Bio-Rad protein assay system (Bio-Rad, Munchen, Germany). 10 µg of protein samples were incubated with 0.5 ml of 2 M Oxalic Acid (Sigma-Aldrich) at 95°C for 30 min. Samples were subsequently centrifuged at 14000 rpm for 5 min. Fluorescence emission in the supernatant was determined spectrofluorimetrically (Glomax, Promega). Excitation and emission wavelengths were set at 405 and 662 nm, respectively. The background was evaluated by measuring fluorescence in non-boiled samples. A standard curve of hemin was run in parallel.

HO Activity Assay

Heme-Oxygenase activity was measured by spectrophotometric determination of bilirubin produced from hemin added as the substrate[7]. Isolated hepatocyts were lysed with a hypotonic buffer (0.1 M potassium phosphate, 2mM $MgCl_2$, Complete Protease Inhibitor Cocktail, Roche Diagnostics Corp., Milano, Italy, pH 7.4) for 15' on ice. After brief sonication. 0.6 M sucrose was added to cell lysates in order to obtain an hysotonic solution (final 0.25 M sucrose). Lysates were centrifuged at 1000 x g for 10 min at 4°C to pellet nuclei, and supernatants centrifuged at 12000 x g for 15 min at 4 °C to pellet mitochondria. Finally, supernatants were ultracentrifuged at 105000 x g for 1 hour at 4°C. Microsomal fractions were resuspended in 100 mM potassium phosphate buffer pH 7.4, containing 2 mM MgCl2 and Complete protease inhibitor. Protein concentration was determined using a small aliquot of these suspensions (Bio-Rad, Munchen, Germany). The microsomal supernatant fraction (cytosol) from the liver of a normal rat served as source of biliverdin reductase. Liver supernatant was prepared fresh from rat liver by homogenization in 0.1 M sodium citrate buffer, pH 5, containing 10% glycerol. HO-1 activity assay was carried out by incubating 600 µg microsome proteins with a reaction mixture containing 1 mM NADPH, 2 mM glucose-6-phosphate, 1U glucose-6-phosphate dehydrogenase (Sigma-Aldrich), 25 µM hemin, 2 mg of rat-liver cytosol and 100 mM potassium phosphate buffer, pH 7.4 (400 µl final volume). The reaction was conducted in the dark for 1h at 37 °C and terminated by placing tubes on ice for 2 min. The amount of bilirubin was determined by the difference in absorption between 464 and 530 nm (extinction coefficient, 40

mM^{-1} cm^{-1} for bilirubin). HO activity was expressed in picomoles of bilirubin formed per milligram microsomal protein per hour.

Biliary excretion study

In gallbladder cannulation experiments mice were anesthetized by intramuscular injection. Body temperature was maintained at 37°C by heating pads. After opening the abdominal cavity, the cystic duct was ligated and an i.v. cathether 24GA (BD Insyte, Spain) attached to a PE-10 tubing (Portex limited, Hythe, UK) inserted in the common bile duct and fixed with an additional ligation. After bile flow equilibration for 10 min, bile was collected into preweighed tubes for 15 min. A bolus of heme (30 µmol/kg body weight) was then infused into the tail vein of mice. Bile was collected through the cannula after heme infusion for 1,15 hr at 15 min intervals and then up to 4.15 at 1hr intervals. Bile flow was determined by weighing the collected bile samples, assuming a density of 1.0 g/ml for bile. Bile samples were frozen immediately and stored at -20°C [8].

In gallbladder removal experiments, mice were intravenously infused with heme (30 µmol/kg body weight) or with SnPP (30 µmol/kg body weight) and 1h later, with heme. After 1, 3 or 5 hours an upper midline laparotomy was realized, the cystic duct was ligated and transected and a cholecystectomy performed. Gallbladder was removed and its volume was determined by water displacement. Bile was collected and stored at -20°C until analysis.

Bilirubin and Heme Concentration in serum and bile

Direct and Total bilirubin concentrations in serum and bile were determined colorimetrically using the QuantiChrom bilirubin assay kit DIBR-180 from BioAssay Systems (Hayward, CA). Heme concentrations in serum were determined colorimetrically using the QuantiChrom Heme assay kit DIHM-250 from BioAssay Systems.

Measurement of Total Bile Acid Concentrations in bile

Total Bile Acid (TBA) concentrations in bile was measured using a total bile acids assay kit according to the procedure supplied by the manufacturer (Diazyme, San Diego, California). The concentration of bile acids is expressed as pmol TBA excreted per min per gram of liver.

Cell culture

HUVECs were isolated from human humbilical vein and cultured in Medium199 (Invitrogen) added with bFGF 10ng/ml, heparin, 20%FBS and 1% penicillin/streptomycin on 0,1% gelatin (Sigma).

Measurement of intracellular ROS accumulation

Accumulation of ROS in HUVECs and aortic rings was assessed by using the oxidant-sensitive fluorescent dye 29,79-dichlorodihydrofluoroscein diacetate (H_2DCFDA; Molecular Probes, Inc., Eugene, OR). H_2DCFDA penetrates easily into the cells. Upon crossing the cellular membrane, H_2DCFDA undergoes deacetylation by intracellular esterases producing a non-fluorescent compound that becomes highly green fluorescent following oxidation by intracellular ROS. Within the cell the probe reacts with ROS to form fluorescent 28,78 dichlorofluoroscein (DCF), which is detected with spectrofluorometry. HUVECs untreated or treated for 20 hrs with 15 µM Hx-heme, HSA-heme or heme alone were incubated with 5µM H_2DCFDA in Hanks' balanced salt solution (HBSS) for 30 min at 37 °C under 5% CO_2 atmosphere. Then cells were washed twice with HBSS, trypsinyzed and analyzed by flow cytometry using a FACS flow cytometer[9].

Similarly, aortic rings from HbA, HbS and Hx-treated HbS mice were incubated with 20µM H_2DCFDA in Krebs-Henseleit buffer for 60 min at 37 °C under 5% CO_2 atmosphere. Fluorescence was recorded at excitation and emission wavelengths of 485 and 530 respectively by a fluorimeter plate reader (Promega). The background fluorescence caused by buffer and DCF was subtracted from the total fluorescence in each well generated by aortic rings in presence of DCF. Fluorescence intensity units were normalized by mg of weight tissue for each aortic rings and expressed as arbitrary fluorescence units/mg tissue[10].

Tissue Iron Measurement

Tissue non-heme iron content determined with a colorimetric method using 4,7-diphenyl-1, 10-phenantroline disulphonic acid (BPS) as chromogen[11]. Briefly, 0.1 g of dry tissue was incubated overnight in a mixture of trichloroacetic (10%) and hydrochloric (4N) acids, and 100 µl of supernatant reduced with thioglycolic acid (Sigma-Aldrich) and acetic acid-acetate buffer (pH4.5). Ferrous iron content was determined spectrophotometrically at 535 nm following addition of BPS and incubation for 1 hr at 37ºC. Results were expressed as µg iron/g dry tissue weight.

LDH Activity Assay

LDH activity in serum was determined colorimetrically using the QuantiChrom Lactate Dehydrogenase kit DLDH-100 from BioAssay Systems. Serum LDH activity was expressed as Unit of LDH(1U/L) catalyzing the conversion of 1 µmole of lactate to pyruvate per minute at pH 8.2.

Echocardiography

Transthoracic echocardiography was performed with a small animal high-resolution imaging system (VeVo2100, VisualSonics, Inc, Toronto, Canad) equipped with a 22-55 MHz trasducer (MicroScan Transducers, MS500D)[12]. The mice, anesthetized by isoflurane (2%) inhalation and maintained by mask ventilation (isoflurane 1%), were placed in a shallow left lateral decubitus position, with strict thermoregulation (37+-1°C) to optimize physiological conditions and reduce hemodynamic variability. Fur was removed from the chest by application of a cosmetic cream to gain a clear image. Echocardiographic parameters were mesured at the level of the papillary muscles in the parasternal short-axis view (M mode). LV fractional shortening was calculated as follows: FS = ((LVEDD - LVESD)/ LVEDD) X 100, where LVFS indicates LV fractional shortening;LVEDD, LV end-diastolic diameter; and LVESD, LV end-systolic diameter. LV ejection fraction was calculated automatically by the echocardiography system. Cardiac output was calculated as the product of stroke volume and heart rate. All measurements were averaged on 5 consecutive cardiac cycles per experiment and cardiac function was assessed when heart rate was 450-500 bpm.

Quantitative Real-Time Polymerase Chain Reaction Analysis

Total RNA was extracted using Pure Link RNA Mini Kit (Ambion, Invitrogen, US). 1μg of total RNA was reverse transcribed by using M-MLV reverse transcriptase (Invitrogen) and random primers (New England Biolabs, Ipswich, MA). qRT-PCR was performed on a 7300 Real Time PCR System (Applied Biosystems, California). Primers and probes were designed using the ProbeFinder software (www.roche-applied-science.com).

Protein Extraction and Western Blotting

Tissue and cell proteins were extracted as previously reported[4] and concentration was determined using the Bio-Rad protein assay system (Bio-Rad, Germany). One μl of plasma or 50μg of total protein extracts were separated on 8/12% SDS-PAGE and analyzed by Western blotting using antibodies against Hx[4], Hp (Sigma H5015), HO-1 (Stressgen, Victoria, Canada)**,** VCAM-1 (R&D, Minneapolis, US), Nitrotyrosine (Millipore,#06-284), L- and H-Ferritin, FPN, eNOS (BD Transduction Lab.), P-eNOS (Cell Signaling), SOD-1 and actin (Santa Cruz).

Histology

Animals were anesthetized and transcardially perfused with PBS. Tissues were collected, fixed in 10% formalin overnight at room temperature and embedded in paraffin. Microtome sections, 5 μm thick, were stained with hematoxylin and eosin.

Supplemental Results

Additional data on Hepatic Heme Metabolism

Regulation of HO-1 expression

We observed that heme accumulated to a significantly lower extent in the liver of heme-overloaded Hx-null mice than in that of wild-type animals. In agreement with liver heme uptake results, ALAS-1 mRNA, which is transcriptionally down-regulated by intracellular heme[34], was decreased in the liver of heme-treated wild-type mice but not in that of Hx-null mice (Figure S1a).

It is likely that heme accumulation in the liver also contributed to HO-1 induction as previous works demonstrated that HO-1 expression is mainly regulated by heme-mediated removal of the repressor Bach1 and binding of the transcriptional factor Nrf2 to HO-1 promoter[32, 33]. Accordingly, we observed an higher amount of Nrf2 in the nuclei of hepatocytes isolated from heme-treated wild-type mice than in those from heme-treated Hx-null animals (Figure S1b) that could account for the enhanced HO protein level found in these mice.

Bilirubin and Heme excretion in the bile

We demonstrated that biliary bilirubin was strongly increased after heme injection in both wild-type and Hx-null mice, with a peak 30-45 minutes after heme injection and this increase was significantly higher in wild-type mice compared to Hx-null animals (Figure S2a). This resulted in a significantly higher amount of bilirubin excreted in the bile of wild-type mice (150 nomoles) compared to Hx-null mice (80 nmoles) in the first four hours after heme injection. A similar difference was observed in heme excreted into the bile. We observed that heme excretion in the bile was significantly higher in heme-overloaded wild-type mice than in Hx-null counterpart (Figure S2b,c) and this resulted in higher amount of heme excreted in the bile in the first four hours after heme injection (40 nmoles in wild-type vs. 15 nmoles in Hx-null).

Bile flow and total bile acid (TBA) excretion were monitored before and after heme infusion. Under basal condition bile flow (Figure S2d) and TBA excretion (not shown) appeared comparable in wild-type and Hx-null mice, thus indicating that biliary excretion was not altered in Hx-deficient animals. In both wild-type mice and Hx-null mice bile flow was not significantly affected by heme treatment. Only Hx-null mice showed a trend toward a slower flow (Figure S2d). Total bile acid excretion was slightly but not significantly decreased in both wild-type mice and Hx-null animals after heme injection (not shown). The slight reduction in bile flow and TBA excretion after heme infusion may occur as a consequence of increased oxidative stress that has been demonstrated to

impair bile excretion. Due to more pronounced alteration in the oxidative status, this effect is more evident in heme-treated Hx-null mice. The observed decrease in TBA excretion could be alternatively due to an increase in the bile acid-independent component of the bile flow versus the bile acid-dependent one.

Thus, our results indicate that the liver heme detoxifying potential is mainly accounted for by HO activity and, to a lesser extent, by biliary heme excretion and both these mechanism are strongly induced following Hx-mediated heme uptake. Putting together the data on catabolism and excretion, we conclude that the presence of Hx in serum increases by two-fold the amount of heme detoxified in the liver.

Contribution of heme catabolism and heme excretion to Hx-mediated heme detoxification

Other than through catabolism, Hx-mediated heme delivery to the liver promotes heme detoxification through direct excretion of the molecule as an intact porphyrin in the bile. Interestingly, we found an inverse correlation between biliary excretion of bilirubin and heme: wild-type mice that excreted less bilirubin showed an increased excretion of intact heme and viceversa (Figure S3a). To evaluate whether heme excretion may be affected by the rate of catabolism, we analyzed biliary excretion of heme in wild-type mice treated with the HO inhibitor Tin-protoporphyrin IX before heme injection. As expected Tin-protoporphyrin IX treatment completely blocked biliary excretion of bilirubin in heme-overloaded wild-type mice (Figure 3b). Moreover, treatment with Tin-protoporphyrin IX resulted in a higher accumulation of heme in the liver of these animals and enhanced excretion of intact heme in the bile (Figure S3c,d), indicating that these two mechanisms of detoxification work together to efficiently remove heme excess.

### NOS expression and activity in the liver of SCD mice

Previous works demonstrated that hemin, thanks to its ability to induce HO-1, is able to attenuate iNOS expression and activity[13, 14]. HO-1 activation can negatively modulate iNOS by releasing CO, which is able to interact with iNOS heme moiety, thus causing its inactivation, and iron, which downregulates iNOS transcription[13, 14]. We demonstrated that Hx treatment of SCD mice resulted in a significantly higher iron accumulation in the liver as well as in an enhanced induction of HO-1 (Figure 6a,b Main Text; Figure S4a). Moreover, we observed that iNOS expression was reduced in the liver of SCD mice after Hx treatment (Figure S4b). Both the enhanced Hx-mediated heme-iron uptake by the liver and the increased HO-1-mediated CO production could account for iNOS downregulation. Even though iNOS expression is increased in the liver of sickle mice and

downregulated after Hx administration, its activity has an opposite modulation, being strongly suppressed in non treated animals and restored after Hx treatment (FureS4c). This observation suggests that iNOS upregulation occurs as an attempt to compensate for the reduced activity of the enzyme, most likely related to oxidative stress and cofactor/substrate consumption. NOS oxidative inactivation is completely prevented by administering the anti-oxidant Hx. The restoration of NOS activity in Hx-treated animals could further contribute to HO-1 upregulation, that in turn may downregulates iNOS expression.

Rescue of the phenotype of Hx-null mice through the administration of purified human Hx

To demonstrate that injected human Hx is able to restore hepatic heme detoxifying potential, we evaluated the ability of human Hx to rescue heme recovery capacity in heme-overloaded Hx-null mice. Hx-null mice were injected with human Hx at physiological concentration 1 h before heme injection and liver heme content and biliary bilirubin and heme were analyzed. As shown in Figure S5, Hx-treated Hx-null mice fully recovered the capacity to take up heme by the liver and to detoxify it (Figure S5a,c,d). Heme uptake by the liver in Hx-treated Hx-null mice was further proved by the modulation of ALAS1 mRNA (Figure S5b).

Supplemental Figures
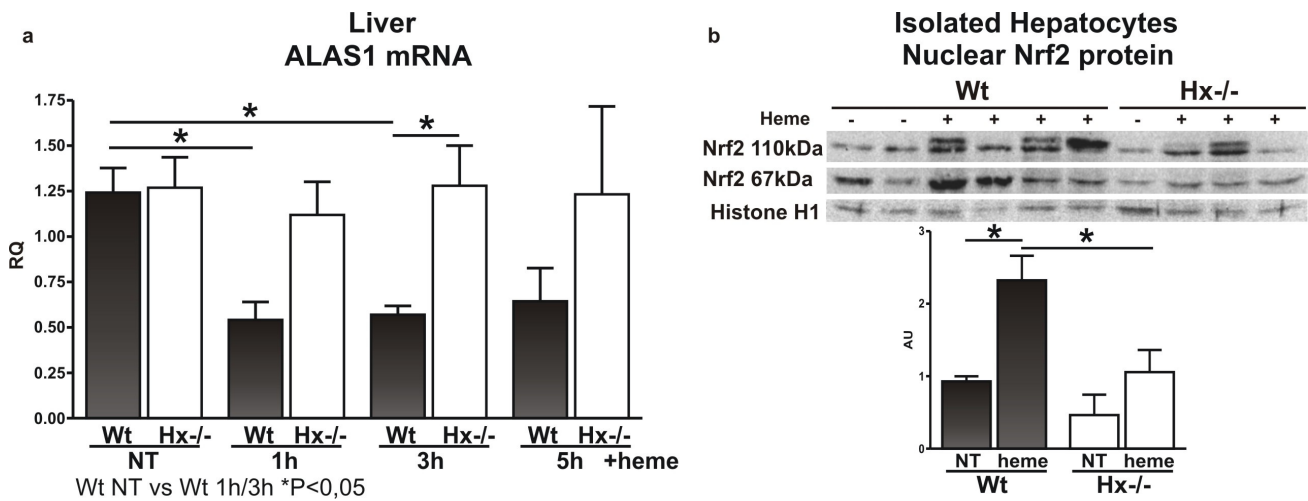
Figure S1. Heme does not accumulate in the liver when Hx is lacking. (a) qRT-PCR analysis of ALAS1 mRNA in the liver of wild-type and Hx-null mice at different time points after heme injection (n=6). (b) Representative Western blots showing nuclear Nrf2 expression in isolated hepatocyte extracts from wild-type and Hx-null mice 6h after heme injection (NT:n=3; heme:n=6). AU: Arbitrary Units. Values represent mean±SEM. *P<0.05.
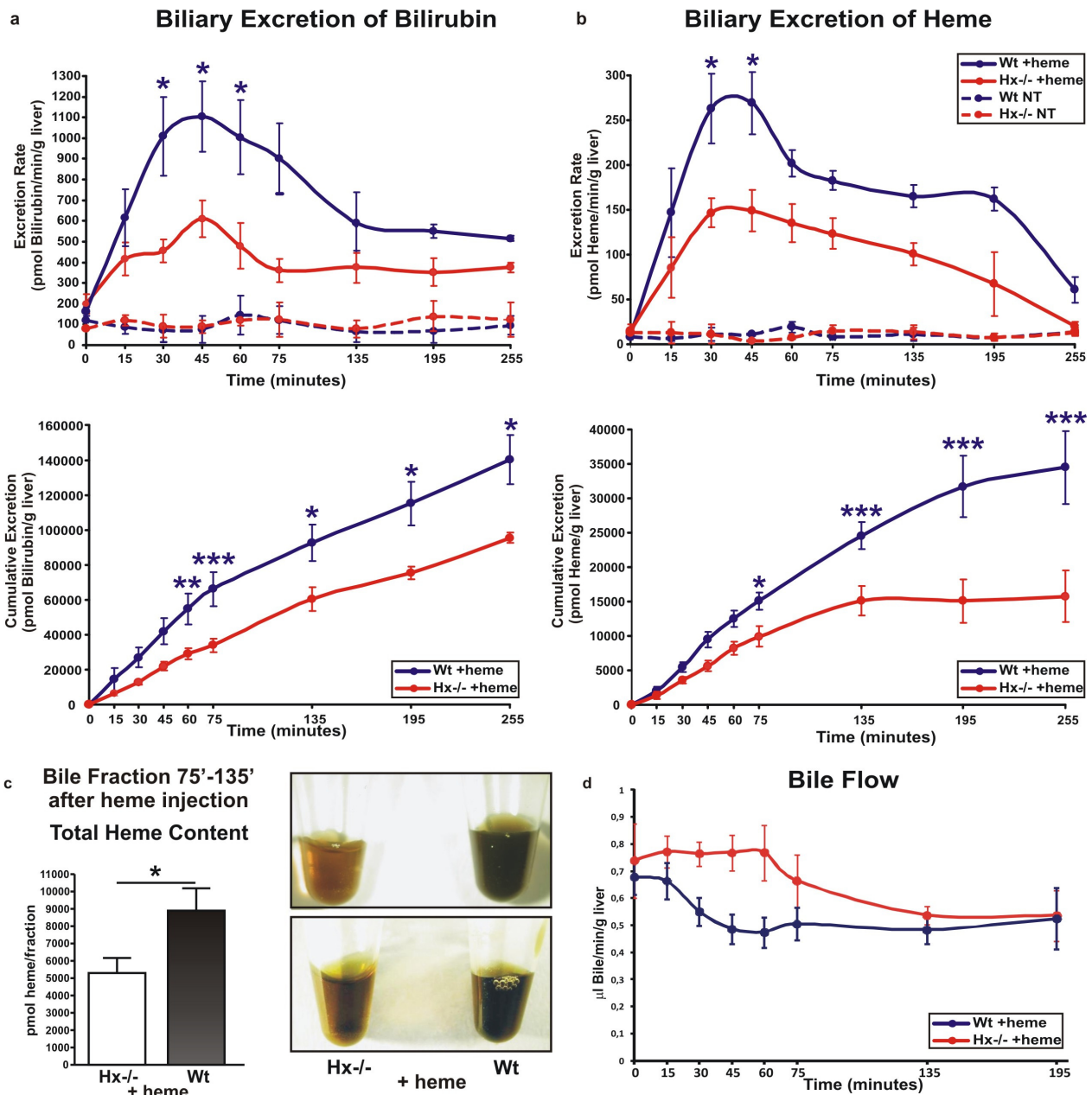
Figure S2. Hx promotes heme detoxification by the liver. (a,b) Excretion rate and cumulative excretion of bilirubin and heme in the bile of heme-overloaded wild-type and Hx-null mice (NT:n=4; heme:n=12). (c) Heme content in the bile fraction 75'-135' of heme-overloaded mice (n=7). Representative fractions of 2 Hx-null and 2 wild-type mice are shown. (d) Bile flow in wild-type and Hx-null mice before (time 0) and at different time points after heme injection (n=12). Values represent mean±SEM. *P<0.05;**P<0.01;***P<0.001.
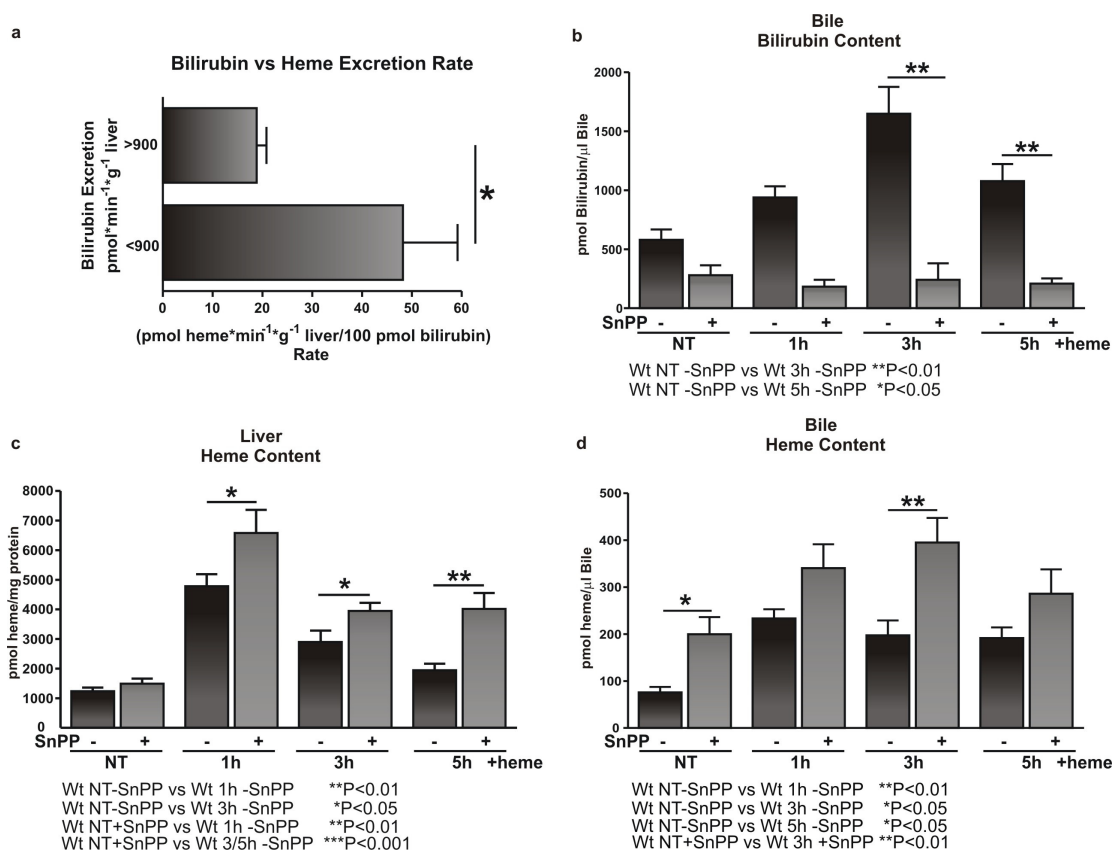
Figure S3. Heme degradation and heme excretion are inversely correlated. (a) Biliary excretion rate of heme plotted on biliary excretion rate of bilirubin. Mice were arbitrarily divided into two groups according to bilirubin excretion (more or less than 900 pmol/min/g liver) (n=4). (b-d) Biliary bilirubin (b) and liver (c) and biliary (d) heme content in Tin-protoporphyrin IX (SnPP)-treated heme-overloaded wild-type mice at different time points after heme injection. Gallbladder was ligated and removed at the indicated time points and bile collected. (Wt -Tin-protoporphyrin IX: n=9; Wt +Tin-protoporphyrin: n=6). Values represent mean ± SEM. *$P<0.05$; **$P<0.01$.

**Hx treatment in Sickle mice**
Liver

a **HO-1 mRNA** b **iNOS mRNA** c **Ca^{2+}-independent NOS Activity Assay**
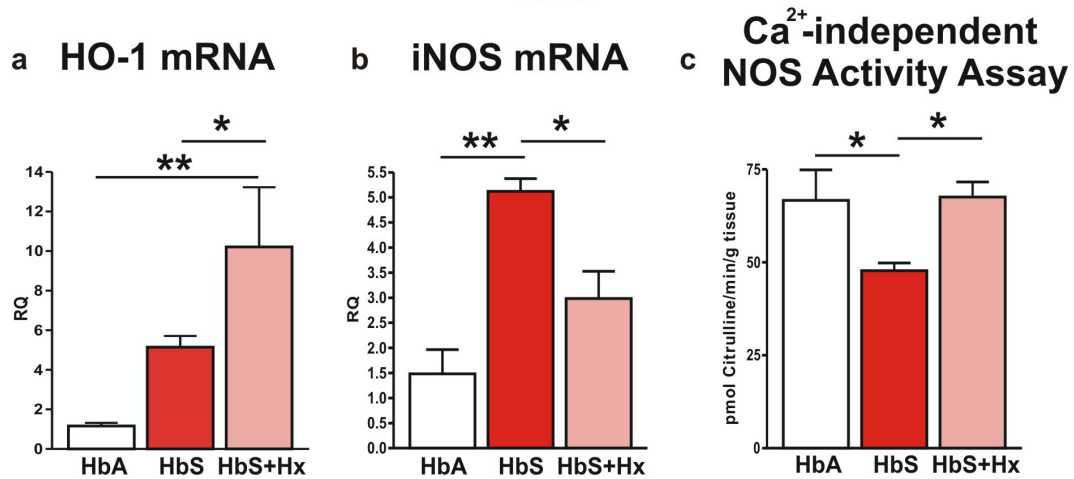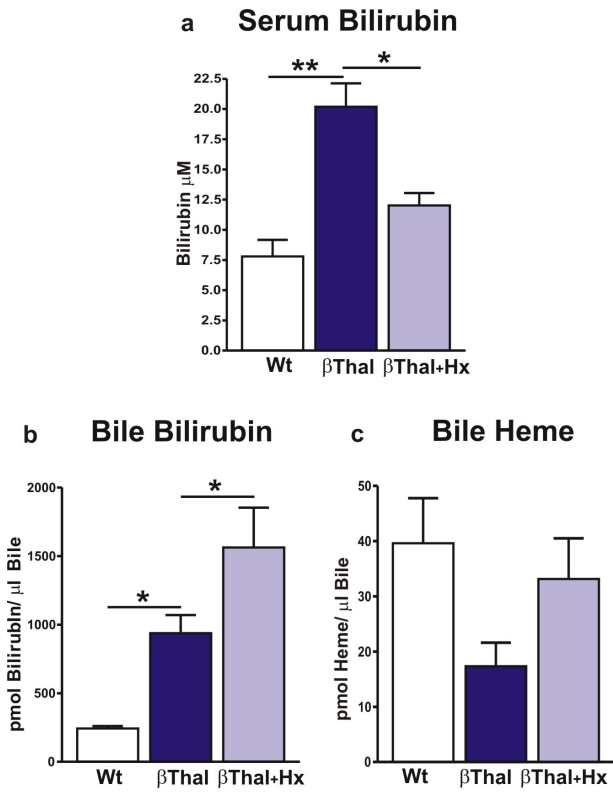
Figure S4. Hx modulates hepatic iNOS expression and activity in SCD mice. (a,b) qRT-PCR analysis of HO-1 and iNOS mRNA level in the liver of HbA, HbS and Hx-treated HbS mice (n=4). (c) Calcium-independent NOS activity in extracts of liver from HbA, HbS and Hx-treated HbS mice. (n=4). Calcium-independent NOS activity assay measures the activity of iNOS, that is the most abundant NOS expressed in the liver. Results shown are representative of three independent experiments. Values represent mean±SEM. *P<0.05;**P<0.01.

Hx-treatment in Hx-null mice

a
Liver
Heme Content

b
Liver
ALAS-1 mRNA

c
Bile
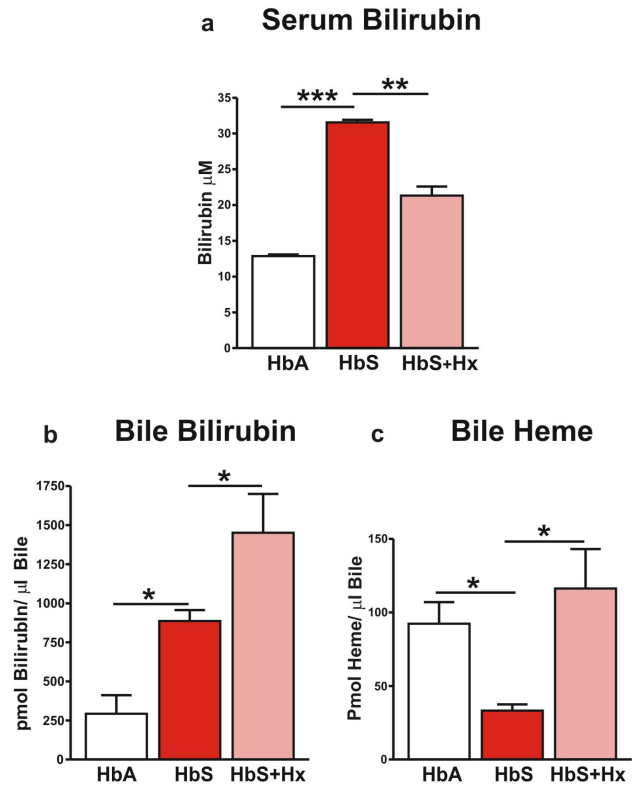### Bilirubin Content

d
Bile
Heme Content
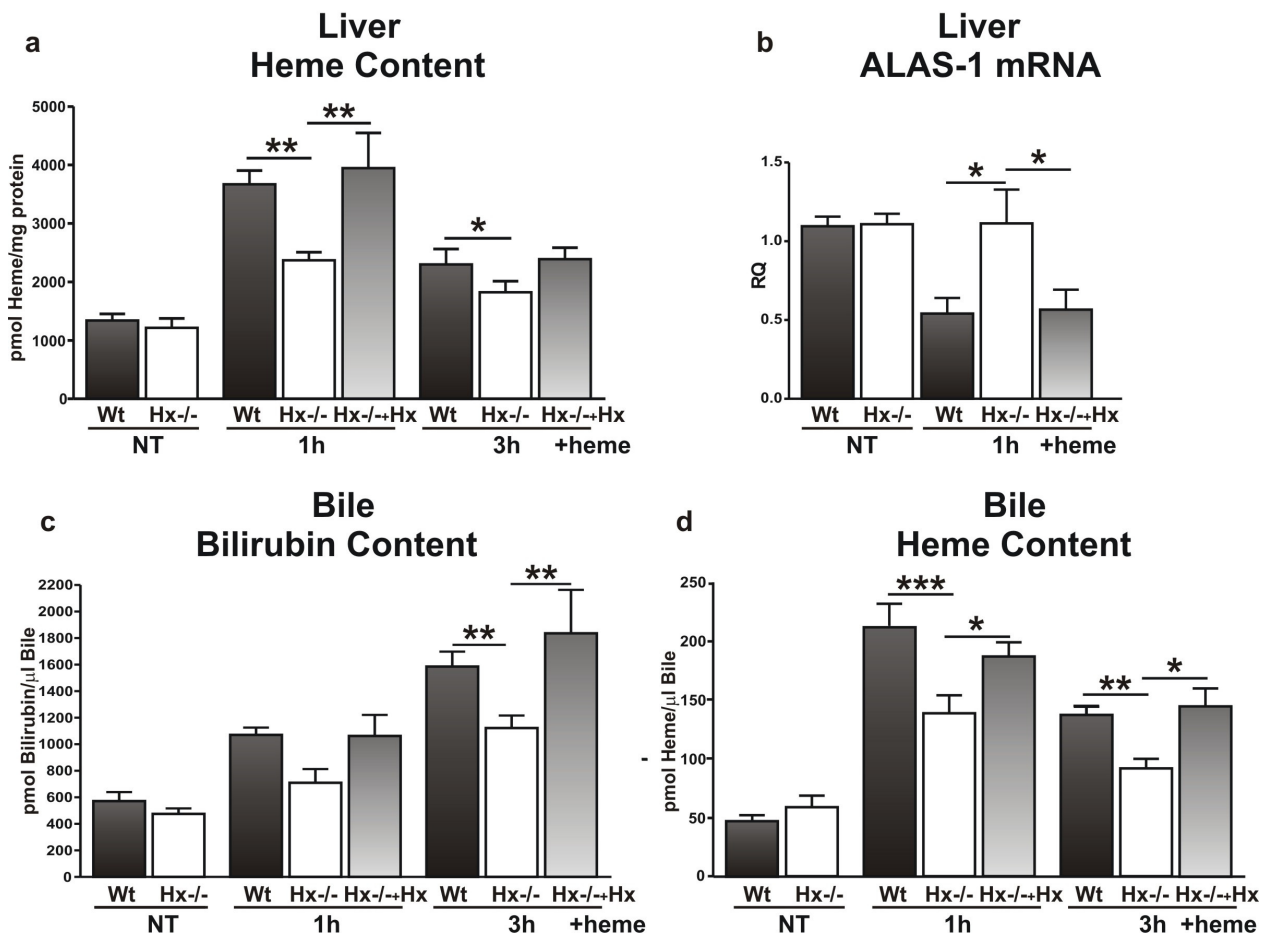
Figure S5. Hx injection in Hx-null mice rescues the hepatic capacity of detoxifying heme. (a) Heme content in the liver of heme-overloaded wild-type mice, Hx-null mice and Hx-treated Hx-null mice at 1 and 3 hours after heme injection. (n=8). (b) qRT-PCR analysis of ALAS1 mRNA in the liver of heme-overloaded wild-type mice, Hx-null mice and Hx-treated Hx-null mice at 1 hour after heme injection (NT: n=4; heme: n=7). (c-d) Bilirubin (c) and heme (d) content in the bile of heme-overloaded wild-type mice, Hx-null mice and Hx-treated Hx-null mice at 1 and 3 hours after heme injection (n=8). Bile was collected after cholecystectomy. Values represent mean ± SEM. *P<0.05; **P<0.01; ***P<0.001. Results shown are representative of three independent experiments.

Figure S6. Hx administration increases biliary bilirubin and heme excretion in thalassemic and SCD mice. Data on wild-type, β-Thal and Hx-treated β-Thal mice and HbA, HbS and Hx-treated HbS mice are shown on the left and right respectively. (a) Serum bilirubin and bile bilirubin (c) and heme content (d) (n=4). Bile was collected after gallbladder ligation. Values represent mean±SEM. *P<0.05; **P<0.01; ***P<0.001. Results shown are representative of three independent experiments.

Sickle mice
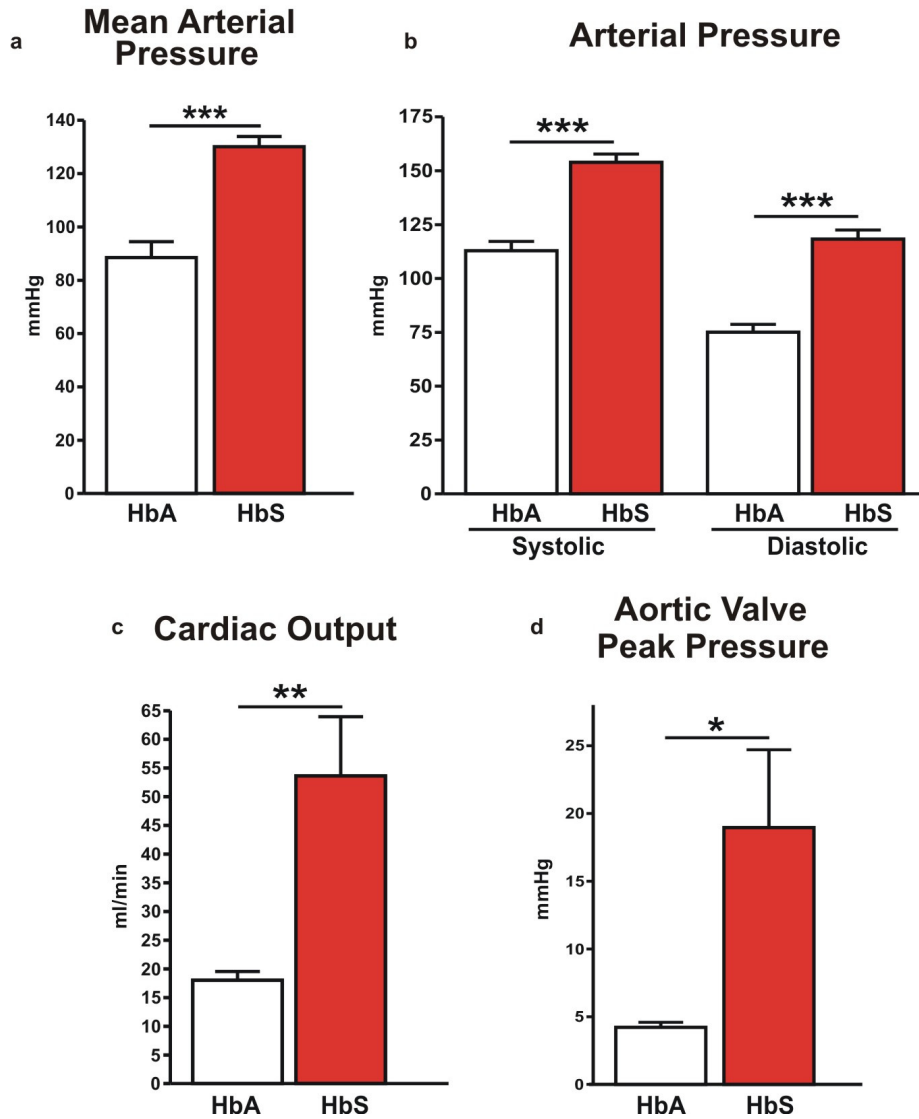
Figure S7. Altered blood pressure and cardiac output in SCD mice. (a) Mean arterial pressure in Hba and Hbs mice. (b) Systolic and diastolic pressure in Hba and Hbs mice. (c,d) Cardiac output and aortic valve peak pressure measured in HbA and HbS mice by echocardiography. HbA n=6; HbS n=10. Results shown are representative of three independent experiments. Values represent mean±SEM. *P<0.05;**P<0.01;***P<0.001.
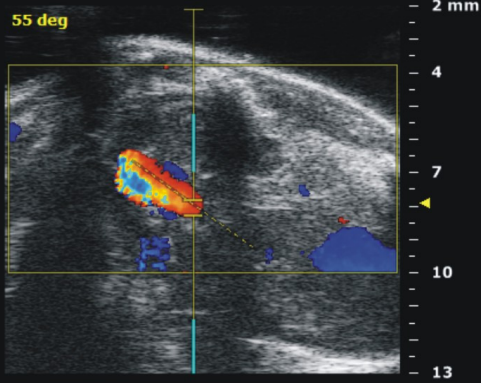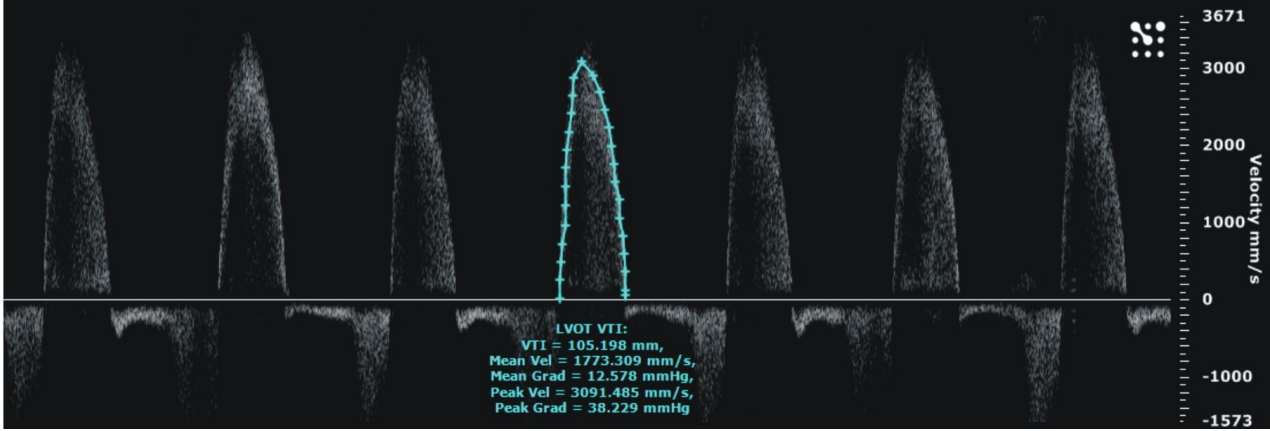
HbA

40 deg
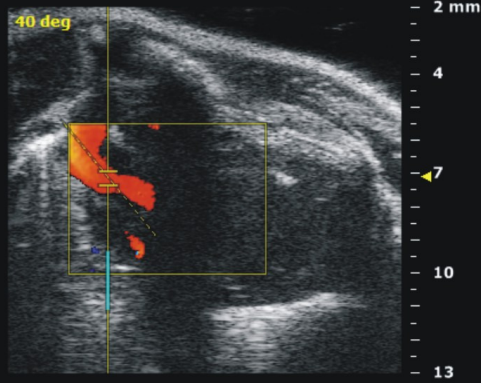
AoV VTI:
VTI = 27.698 mm,
Mean Vel = 536.008 mm/s,
Mean Grad = 1.149 mmHg,
Peak Vel = 942.968 mm/s,
Peak Grad = 3.557 mmHg

HbS

55 deg
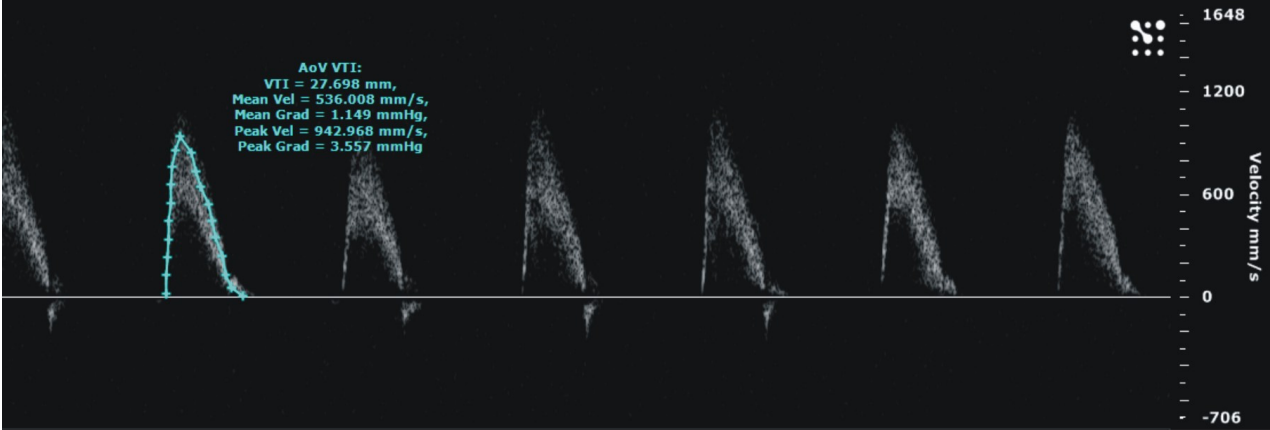
LVOT VTI:
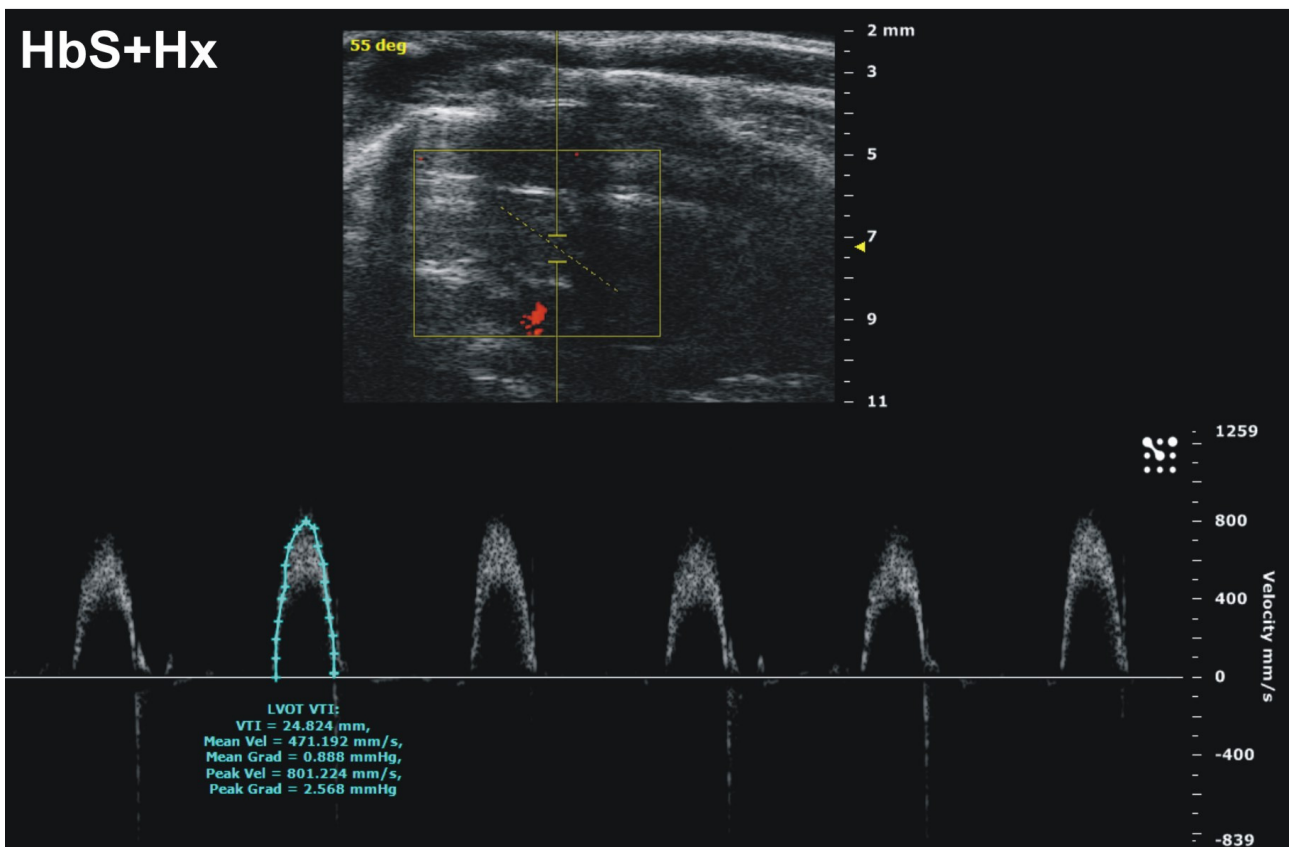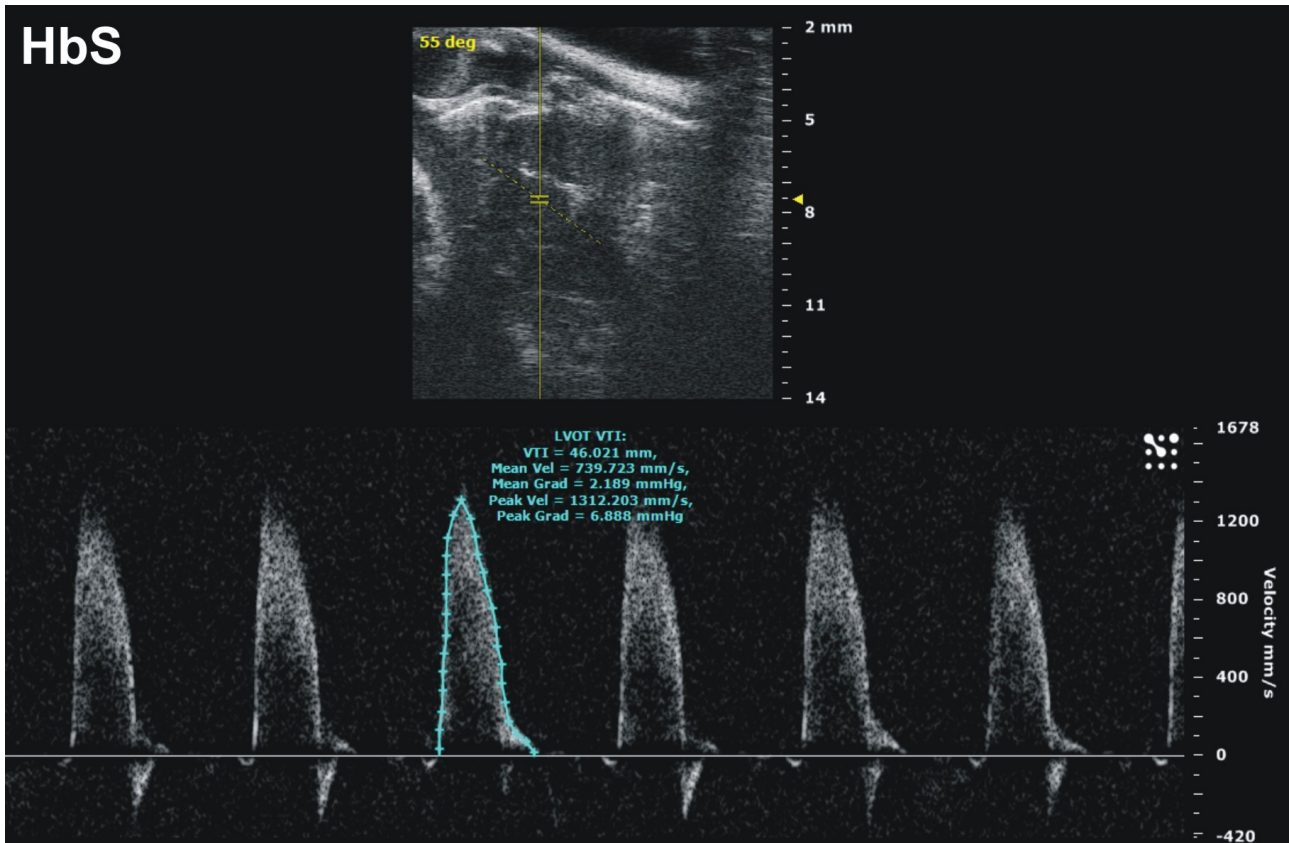VTI = 105.198 mm,
Mean Vel = 1773.309 mm/s,
Mean Grad = 12.578 mmHg,
Peak Vel = 3091.485 mm/s,
Peak Grad = 38.229 mmHg

Figure S8. Pulsed wave Doppler on the left ventricular outflow (LVOT) in HbA, HbS and Hx-treated HbS mice. The velocitiy time interval (VTI) was measured for inclusion in the CO calculation. VTI was higher in HbS mice compared to HbA mice and restored after Hx treatment.

Supplemental Tables

Table S1. Statistic Analysis. Table showing the statistic tests used for each panel of each figure. On the right it is reported the total number of comparisons that was applied for each Bonferroni adjustment

Figure number (panel)	Test	N. of comparisons
Figure 1 (a,b,c,d,e,f,g,h)	Welch T-test	2
Figure 2 (a,b,c,d,e,f,g,h,i,l)	Two-way ANOVA	2+2 = 4
Figure 3 (a)	Two-way ANOVA (between Hx-heme and HSA-heme)	3+3+3 = 9
Figure 3 (b,d,e,f,g,i,m)	One-way ANOVA	3
Figure 3 (c,h,l)	Two-way ANOVA	2+2+2 = 6
Figure 3 (n)	Welch T-test	1
Figure 4 (a)	Two-way ANOVA	4+3+3 = 10
Figure 4 (b,e)	Two-way ANOVA	3+2+2 = 7
Figure 4 (c)	One-way ANOVA	3
Figure 4 (d,f)	Two-way ANOVA	2+2 = 4
Figure 5 (a,b,c,d,e,f,g,h)	One-way ANOVA	3
Figure 6 (a,b,c,d,e)	One-way ANOVA	3
Figure 7 (a)	Two-way ANOVA RM (between HbS and Hx-treated HbS)	4+4+4=12
Figure 7 (b,c,e,f,g)	One-way ANOVA	3
Figure S1(a)	Two-way ANOVA	4+3+3 = 10
Figure S1(b)	Two-way ANOVA	2+2 = 4
Figure S2 (a,b)	Two-way ANOVA RM (between Wt+heme and Hx-/- +heme)	9
Figure S2 (c)	Welch T-test	2
Figure S2 (d)	Two-way ANOVA RM (between Wt+heme and Hx-/- +heme)	8
Figure S3(a)	Welch T-test	1
Figure S3 (b,c,d)	Two-way ANOVA	4+3+3 = 10
Figure S4 (a,b,c)	One-way ANOVA	3
Figure S5(a,b,c,d)	One-way ANOVA (between Wt+heme, Hx-/-+heme and Hx-/-+heme +Hx, per each time point)	3
Figure S6 (a,b,c)	One-way ANOVA	3
Figure S7 (a,b,c,d)	Welch T-test	2
Table S2, S3	One-way ANOVA	3

.

Table S2. Hx treatment does not recover anemia. Analysis of blood samples from wild-type, β-Thal and Hx-treated β-Thal mice and from HbA, HbS and Hx-treated HbS mice (n=6). Values represent mean ± SEM. WBC: white blood cells; RBC: red blood cells; HGB: hemoglobin; HCT: hematocrit; MCV: mean corpuscular volume; Retic: reticolocytes. *P<0.05.

Blood Analysis

Parameter	Wild-type	Thal	Thal + Hx
WBC (*10^{3}cells/μl)	1.37 ± 0.15	4.53 ± 0.57	3.34 ± 0.18 *P<0,05
RBC (*10^{6}cells/ml)	9.53 ± 0.22	7.25 ± 0.18	7.12 ± 0.08
HGB (g/dl)	13.9 ± 0.26	7.42 ± 0.23	7.4 ± 0.1
HCT (%)	45.4 ± 1.15	29.92 ± 0.73	28.9 ± 0.7
MCV (fL)	47.53 ± 0.42	41.35 ± 0.77	40.63 ± 0.81
Retic (%)	3.28 ± 0.47	22.75 ± 0.93	21.27 ± 0.34

N=5 for each genotype

Parameter	HbA	HbS	HbS + Hx
WBC (*10^{3}cells/μl)	7.48 ± 1.36	17.11 ± 0.88	9.8 ± 0.2 *P<0,05
RBC (*10^{6}cells/ml)	12.37 ± 0.01	4.68 ± 0.12	4.65 ± 0.25
HGB (g/dl)	12.3 ± 0.3	5.56 ± 0.13	5.45 ± 0.25
HCT (%)	51.15 ± 3.15	24.9 ± 0.6	24.75 ± 0.25
MCV (fL)	41.3 ± 2.6	54.25 ± 1.95	51.15 ± 1.15
Retic (%)	10.26 ± 5.47	71.7 ± 3.7	70.35 ± 1.35

N=5 for each genotype

Table S3. Echocardiographic and Hemodynamic Parameters in HbA, HbS and Hx-treated HbS mice.

Parameter	HbA	HbS	HbS + Hx
HR (bpm)	710 ± 36	671 ± 7.63	714 ± 32
FS (%)	43.42 ± 2.4	40.76 ± 3.0	39.71 ± 3.25
EF (%)	75.28 ± 2.43	71.49 ± 3.29	71.04 ± 4.2
IVSTD (mm)	0.93 ± 0.06	1.218 ± 0.048 **	1.099 ± 0.11
IVSTS (mm)	1.40 ± 0.07	1.839 ± 0.097 **	1.682 ± 0.11
LVEDD (mm)	3.32 ± 0.11	3.591 ± 0.129	3.50 ± 0.16
LVESD (mm)	1.89 ± 0.12	2.142 ± 0.155	2.12 ± 0.22
LPWTD (mm)	0.94 ± 0.05	1.164 ± 0.056 *	1.13 ± 0.06
LPWTS (mm)	1.32 ± 0.05	1.645 ± 0.086 *	1.49 ± 0.08
CO (ml/min)	18.04 ± 1.49	55.32 ± 12.3 **	23.29 ± 9.5 #
AV Peak Press (mmHg)	4.22 ± 0.37	16.97 ± 6.02 *	6.4 ± 2.61 #
LV MPI	1.02 ± 0.11	0.72 ± 0.08 *	0.90 ± 0.11
LVW/BW (mg/g)	3.94 ± 0.14	5.64 ± 0.47 *	5.26 ± 0.25

HR, heart rate; bpm, beats per minute; FS, percent fractional shortening; EF, precent ejection fraction; IVSTD, interventricular septum thickness in end diastole; IVSTD, interventricular septum thickness in end systole; LVEDD, left ventricle end diastolic diameter; LVESD, left ventricle end systolic diameter; LPWTD, left posterior wall thickness in end diastole; LPWTS, left posterior wall thickness in end systole; CO, cardiac output; AV Peak Press, aortic valve peak pressure; LV MPI, left ventricular myocardial performance index; LVW, left ventricular weight; BW, body weight.
* $P<0.05$; **$P<0.01$ HbS versus HbA mice
# $P<0.05$ HbS+Hx versus HbS mice

Older HbS mice (8-12 month-old) showed right ventricule dilation and developed pulmonary hypertension, accordingly to what occur in the human sickle cell disease[15, 16].

Supplemental References

1.	De Franceschi L, Daraio F, Filippini A, Carturan S, Muchitsch EM, Roetto A, Camaschella C. Liver expression of hepcidin and other iron genes in two mouse models of beta-thalassemia. *Haematologica.* 2006;91:1336-1342.
2.	Ryan TM, Ciavatta DJ, Townes TM. Knockout-transgenic mouse model of sickle cell disease. *Science.* 1997;278:873-876.
3.	Wu LC, Sun CW, Ryan TM, Pawlik KM, Ren J, Townes TM. Correction of sickle cell disease by homologous recombination in embryonic stem cells. *Blood.* 2006;108:1183-1188.
4.	Vinchi F, Gastaldi S, Silengo L, Altruda F, Tolosano E. Hemopexin prevents endothelial damage and liver congestion in a mouse model of heme overload. *Am J Pathol.* 2008;173:289-299.
5.	Goncalves LA, Vigario AM, Penha-Goncalves C. Improved isolation of murine hepatocytes for in vitro malaria liver stage studies. *Malar J.* 2007;6:169.
6.	Sassa S. Sequential induction of heme pathway enzymes during erythroid differentiation of mouse Friend leukemia virus-infected cells. *J Exp Med.* 1976;143:305-315.
7.	Marinissen MJ, Tanos T, Bolos M, de Sagarra MR, Coso OA, Cuadrado A. Inhibition of heme oxygenase-1 interferes with the transforming activity of the Kaposi sarcoma herpesvirus-encoded G protein-coupled receptor. *J Biol Chem.* 2006;281:11332-11346.
8.	Lam P, Wang R, Ling V. Bile acid transport in sister of P-glycoprotein (ABCB11) knockout mice. *Biochemistry.* 2005;44:12598-12605.
9.	Eruslanov E, Kusmartsev S. Identification of ROS using oxidized DCFDA and flow-cytometry. *Methods Mol Biol.*594:57-72.
10.	El-Awady MS, Ansari HR, Fil D, Tilley SL, Mustafa SJ. NADPH oxidase pathway is involved in aortic contraction induced by A3 adenosine receptor in mice. *J Pharmacol Exp Ther.*338:711-717.
11.	Pieroni L, Khalil L, Charlotte F, Poynard T, Piton A, Hainque B, Imbert-Bismut F. Comparison of bathophenanthroline sulfonate and ferene as chromogens in colorimetric measurement of low hepatic iron concentration. *Clin Chem.* 2001;47:2059-2061.
12.	Ghigo A, Perino A, Mehel H, Zahradnikova A, Jr., Morello F, Leroy J, Nikolaev VO, Damilano F, Cimino J, De Luca E, Richter W, Westenbroek R, Catterall WA, Zhang J, Yan C, Conti M, Gomez AM, Vandecasteele G, Hirsch E, Fischmeister R. Phosphoinositide 3-Kinase gamma Protects Against Catecholamine-Induced Ventricular Arrhythmia Through Protein Kinase A-Mediated Regulation of Distinct Phosphodiesterases. *Circulation.* 2012;126:2073-2083.
13.	Sheng WS, Hu S, Nettles AR, Lokensgard JR, Vercellotti GM, Rock RB. Hemin inhibits NO production by IL-1beta-stimulated human astrocytes through induction of heme oxygenase-1 and reduction of p38 MAPK activation. *J Neuroinflammation.* 2010;7:51.
14.	Datta PK, Koukouritaki SB, Hopp KA, Lianos EA. Heme oxygenase-1 induction attenuates inducible nitric oxide synthase expression and proteinuria in glomerulonephritis. *J Am Soc Nephrol.* 1999;10:2540-2550.
15.	Lee MT, Rosenzweig EB, Cairo MS. Pulmonary hypertension in sickle cell disease. *Clin Adv Hematol Oncol.* 2007;5:645-653, 585.
16.	Voskaridou E, Christoulas D, Terpos E. Sickle-cell disease and the heart: review of the current literature. *Br J Haematol.*157:664-673.